N-donor Base Adducts of P_2O_5 as Diphosphorylation Reagents

Scott M. Shepard and Christopher C. Cummins*
Department of Chemistry, Massachusetts Institute of Technology, Cambridge MA
Received June 23, 2021; E-mail: ccummins@mit.edu

Abstract:

Diphosphorylation of select nucleophiles was achieved by treatment with neutral, doubly zwitterionic adducts of nucleophilic N-donor bases (pyridine, DABCO) and P_2O_5. Treatment of the PPN salt of TriMP with TsCl and triethylamine yielded a mixed PPN and triethylammonium salt of tosyl TriMP ([PPN][HNEt$_3$][P$_3$O$_9$Ts], **1**), isolated in 55% yield and crystallographically characterized. Treatment of **1** with two equivalents of DABCO led in situ to an unisolated ring opened intermediate, an adduct of two DABCO molecules and $(P_3O_8)^-$ ([DABCO-P$_3$O$_8$-DABCO]$^-$, **2**). Reaction of **2** with additional DABCO results in precipitation of a neutral, doubly zwitterionic adduct of DABCO and P_2O_5 (DABCO-P$_2$O$_5$-DABCO, **3**). Compound **3** is more conveniently prepared by treatment of polymeric phosphorus pentoxide ($(P_2O_5)_\infty$) with DABCO in acetonitrile. Both syntheses also result in an inseparable neutral triply zwitterionic impurity, an adduct of three molecules of DABCO and P_4O_{10} (P_4O_{10}(DABCO)$_3$, **4**). Both **3** and **4** were crystallographically characterized by careful selection of crystals for X-ray diffraction. A similar neutral, doubly zwitterionic adduct of pyridine and P_2O_5 (Pyr-P$_2$O$_5$-Pyr, **5**) was prepared by treatment of $(P_2O_5)_\infty$ with pyridine in 77% yield. Due to higher purity, **5** was used for further reactivity studies. Compound **5** reacts with DBU (**6**, 65% yield), diethylamine (**7**, 77% yield), and methanol (**8** and **9**) to producing the corresponding difunctionalized pyrophosphate derivatives. Compound **5** also reacts with the TBA salt of AMP to produce adenosine-substituted TriMP (**10**) as an intermediate that was ring opened with water, diethylamine, and the TBA salt of UMP, yielding ammonium salts of ATP (**11**, 89% yield), γ-diethylamino-ATP (**12**, 58% yield), and adenosine uridine tetraphosphate (**13**, 74% yield) after purification by AX-HPLC. Similarly, adenosine tetraphosphate (**14**) was prepared in 40% yield by treatment of **5** with ADP and hydrolysis of the resulting intermediate.

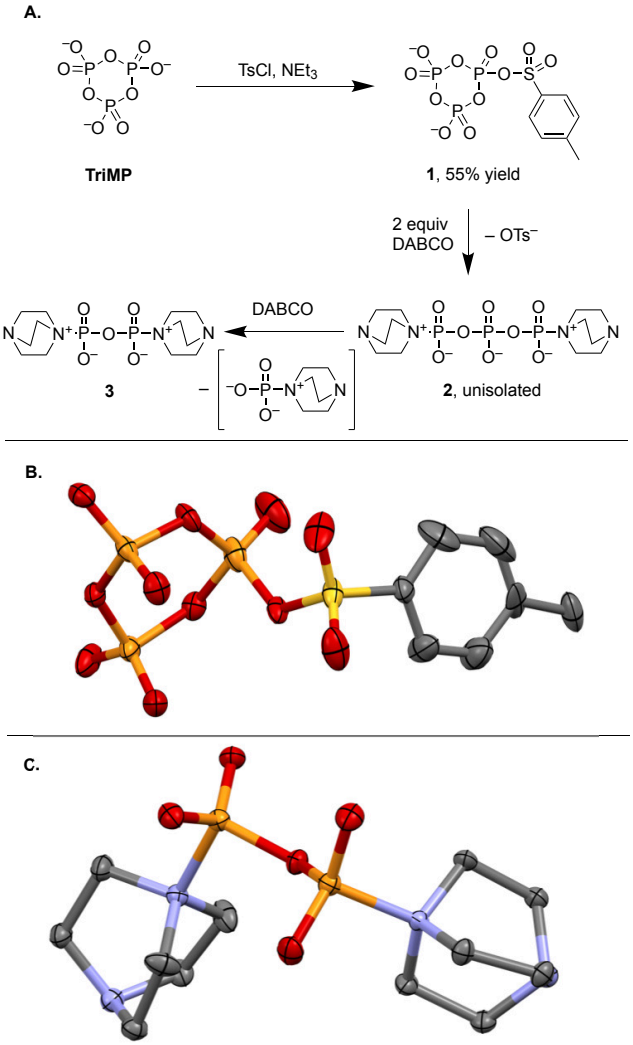

Figure 1. A. Synthesis of tosyl TriMP, **1**, from TriMP and treatment with DABCO to form **3** through unisolated intermediate **2**. B. X-ray crystal structure of **1** with thermal ellipsoids set at 50% probability and cations omitted (red for oxygen, orange for phosphorus, yellow for sulfur, grey for carbon). C. X-ray crystal structure of **3** with thermal ellipsoids set at 50% probability and cations omitted (red for oxygen, orange for phosphorus, blue for nitrogen, grey for carbon).

The last several years have seen an explosion of new reagents and methodologies for the synthesis of oligophosphorylated molecules, due to their prevalence in biological systems.[1–6] This field has slowly developed since Khorana's pioneering first synthesis of adenosine triphosphate (ATP) in 1954,[7] and an improved synthesis of ATP and of other nucleoside triphosphate (NTP) derivatives has been a major area of focus in synthetic oligophosphorylation.[8] Many of the recent developments have focused on reagents for the simultaneous addition of three phosphate units, via trimetaphosphate ($(P_3O_9)^{3-}$, TriMP) in order to minimize the number of synthetic steps to convert a nucleoside into an NTP.[9] The first effective TriMP based methodology was that of Taylor, utilizing the activation of TriMP with sulfonyl chloride reagents.[4,10–13] These seminal papers have been followed up more recently with our own group's[1] as well as Jessen's[3,14] isolable triphosphorylation reagents. By utilizing substrates such as nucleosides, nucleoside monophosphates, and nucleoside diphosphates, these reagents are able to add three phosphate units to form nucleoside triphosphates, tetraphosphates, and pentaphosphates, respectively. Our group has sought to further expand this methodology of well defined, isolable oligophosphorylation reagents to introduce a varying number of phosphate units in one transformation. To that end, we have reported a tetraphosphorylation reagent[15]

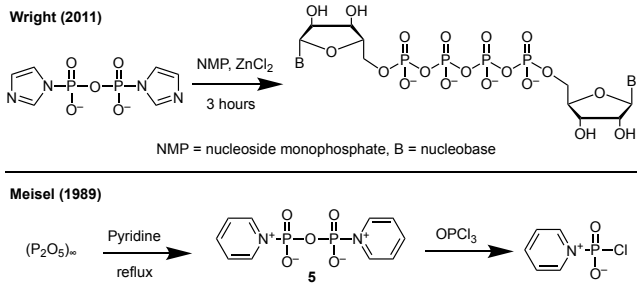

Figure 2. Previous syntheses and reactivities of a dianionic adduct of P_2O_5 and imidazole by Wright[17] and a neutral doubly zwitterionic adduct of P_2O_5 and pyridine by Meisel.[18]

and its utility to synthesize nucleoside tetra- and pentaphosphates.[2,16] Here we further develop this strategy by reporting a potent diphosphorylation reagent and subsequent synthesis of NTP derivatives, a dinucleoside tetraphosphate, and a nucleoside pentaphosphate.

The current investigation began by repeating the earlier triphosphorylation work of Taylor where the TBA (tetrabutylammonium) salt of TriMP is activated with mesitylenesulfonyl chloride and nucleophilic N-donor bases, such as DABCO (1,4-diazabicyclo[2.2.2]octane), pyridine, and *N*-methylimidazole.[4,10–13] The putative mesitylenesulfonyl TriMP species was unisolated in Taylor's reports. However, in an analogous reaction of the PPN (bis(triphenylphosphine)iminium) salt of TriMP and tosyl chloride we were able to isolate and crystallographically characterize tosyl TriMP (**1**, Figure 1). Performing this reaction in dried acetone under anhydrous conditions results in precipitation of anhydrous crystals of a mixed PPN and triethylammonium salt of **1**.

Taylor's phosphorylation methodology additionally involves several amine additives, notably DABCO.[11–13] Treating TriMP with tosyl chloride and DABCO in a one pot procedure gives a complex mixture of products (see S2.3), but isolated **1** reacts cleanly with two equivalents of DABCO to form a ring opened species, an adduct of $(P_3O_8)^{3-}$ and two DABCO molecules (**2**, Figure 1A), as determined by $^{31}P\{^1H\}$ NMR. The utility of **1** and **2** as phosphorylation reagents is however hindered by their instability. Even in the crystalline state at −35 °C, **1** shows significant decomposition to a complex mixture after two weeks, and we were unable to isolate **2** without decomposition to a complex mixture of species (See SI).

Serendipitously, an acetonitrile solution of **2** in the presence of excess DABCO formed colorless crystals upon standing overnight. An X-ray diffraction study of these crystals revealed a neutral, doubly zwitterionic adduct of P_2O_5 and two molecules of DABCO (**3**, Figure 1C). The structure of **3** shows a P–N bond distance of 1.84 Å, in close agreement with an expected P–N single bond length of 1.82 Å.[19] Formation of **3** by reaction of **2** with DABCO formally produces an equivalent of the monoanionic adduct of DABCO and $[PO_3]^-$. However, $^{31}P\{^1H\}$ NMR of the supernatant solution after precipitation of **3** shows a complex mixture of oligophosphate species. The corresponding quinuclidine adduct of metaphosphate has been transiently observed in aqueous solution by $^{31}P\{^1H\}$ NMR and was found to rapidly convert to TriMP.[20] However, TriMP is not a significant component of the mixture of phosphates we observed. Additionally, **3** is only poorly soluble in dichloromethane and chloroform, but $^{31}P\{^1H\}$ NMR spectroscopy indicated the

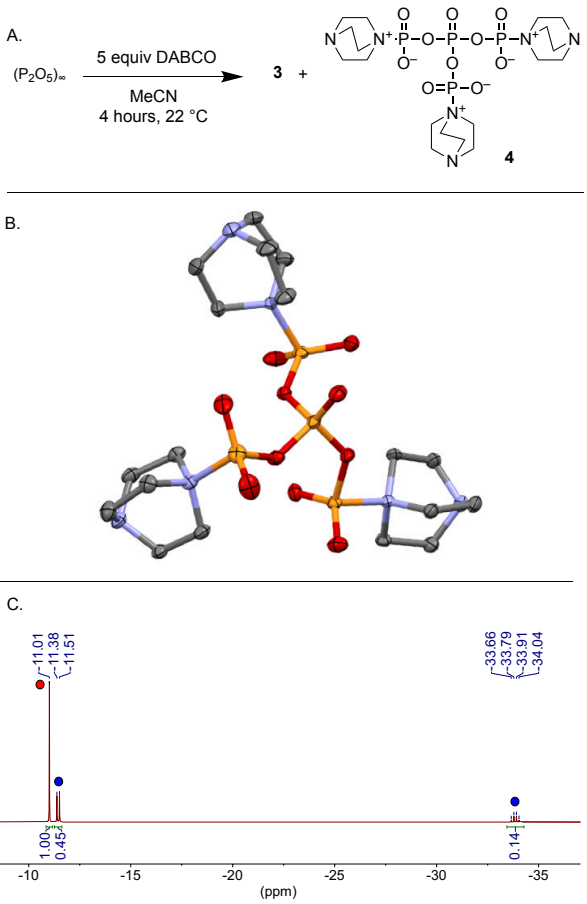

Figure 3. A. Treatment of polymeric $(P_2O_5)_\infty$ with excess DABCO yielded a mixture of **3** and **4**. B. X-ray crystal structure of **4** with thermal ellipsoids set at 50% probability (red for oxygen, orange for phosphorus, blue for nitrogen, grey for carbon). C. $^{31}P\{^1H\}$ NMR (MeCN, 162 MHz) of a mixture of **3** (red) and **4** (blue).

presence of an impurity which we assigned as **4** but were unable to separate (see below, Figure 3). Interested in the potential phosphorylation reactivity of **3**, we sought to develop an easy and large scale synthesis of of this compound for further reactivity studies.

A dianionic bis-phosphorimidazolide has been reported by Wright and is facilely prepared by treatment of pyrophosphate with carbonyldimidazole (CDI) (Figure 2).[17] This compound has been investigated for diphosphorylation activity, but imidazole groups are only moderate leaving groups. Nevertheless, the imidazole adduct reacts slowly with nucleoside monophosphates, a reaction that is greatly accelerated in the presence of promoters such as $ZnCl_2$, to give symmetric dinucleoside tetraphosphates (Figure 2). The only previous report of a neutral doubly zwitterionic adduct of P_2O_5 and an N-donor base is the pyridine adduct reported by Meisel,[18] (**5**) generated by refluxing phosphorus pentoxide ($(P_2O_5)_\infty$) in pyridine (Figure 2). However, this putative pyridine adduct was not characterized or investigated for phosphorylation reactivity. We therefore sought to characterize this pyridine adduct and adapt this synthetic method to **3**. Notably, Wright patented their bis-phosphorimidazolide compound and included the pyridine adduct, **5**, as well as a proposed N-methylimidazole adduct in their application.[21] However, they do not appear to have actually synthesized or explored the reactivity of either of

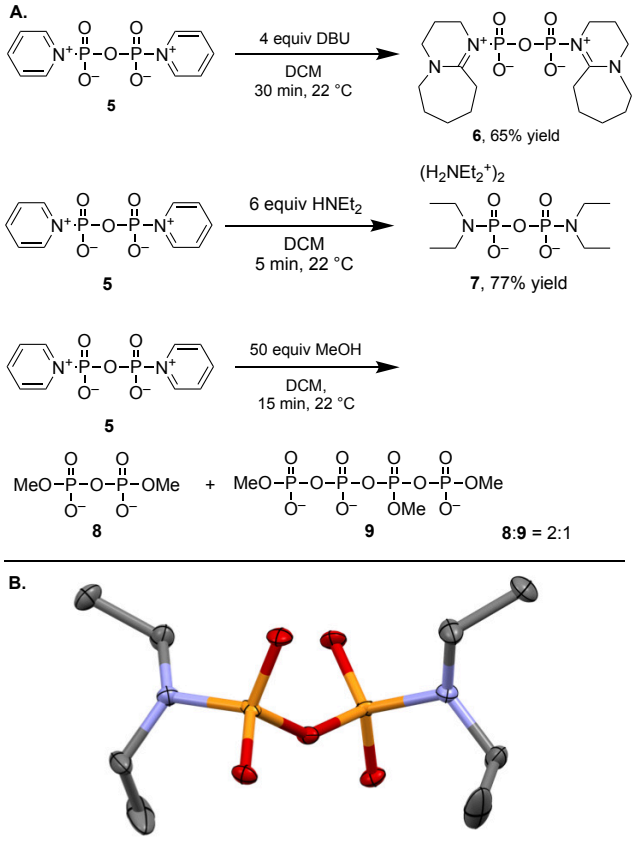

Figure 4. A. Treatment of **5** with DABCO or DBU yields a mixture of **3** and **4** or **6** respectively. Treatment of **5** with a small excess of diethylamine, yielded the diethylammonium salt of **7**. Treating a mixture of **3** and **4** with methanol yields a mixture of **8** and **9**. B. X-ray crystal structure of **7** with thermal ellipsoids set at 50% probability and cations omitted (red for oxygen, orange for phosphorus, blue for nitrogen, grey for carbon).

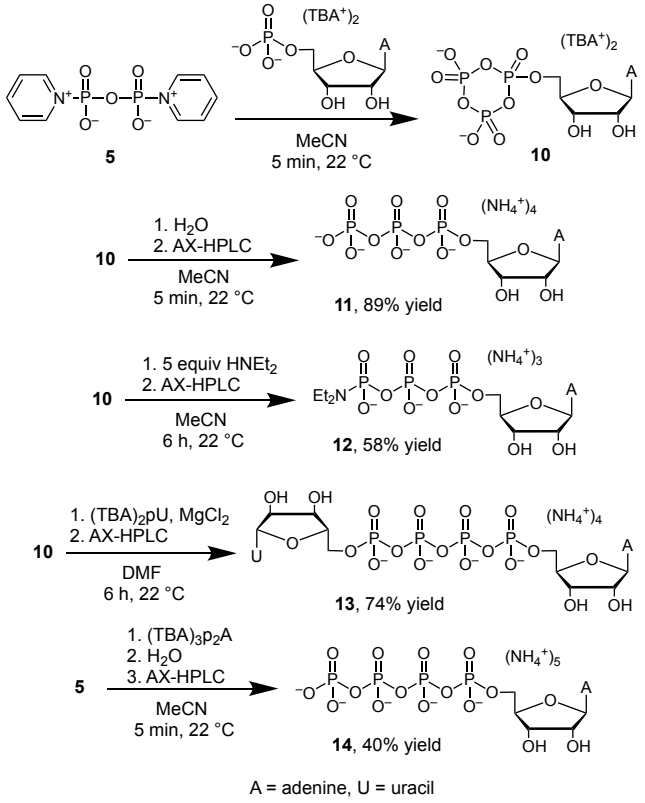

Figure 5. Treatment of **5** with the TBA salt of AMP yielded adenosine-TriMP intermediate **10**. In a one pot procedure from **5**, intermediate **10** was ring opened with water, diethylamine, and the TBA salt of UMP, yielding ammonium salts of **11**, **12**, and **13** after purification by AX-HPLC. Treatment of **5** with the TBA salt of ADP and ring opening with water yields **14**. Yields are reported relative to **5**.

these compound.

Treatment of a suspension of $(P_2O_5)_\infty$ in acetonitrile with excess DABCO leads to rapid formation of a precipitate consisting of a mixture of **3** and **4** (Figure 3A). Conducting this reaction at suitable dilution results in slow precipitation of crystalline solids and the ability to filter out any insoluble impurities. However, the resulting product was always found to be a mixture of **3** and **4**. Extensive attempts to vary conditions or effect purification of the mixture resulted in limited impact on the ratio of the two products. However, careful selection of a crystal for X-ray diffraction provided structural analysis of **4** (Figure 3B), validating our initial assignment of this impurity. Both **3** and **4** can be viewed as two different neutral building blocks of $(P_2O_5)_\infty$ that have been cut out of the polymeric structure[22] by DABCO.

Due to our inability to purify **3**, we turned our investigation to Meisel's[18] analogous pyridine adduct, **5** (Figure 4). Heating $(P_2O_5)_\infty$ and pyridine in acetonitrile to near reflux for 24 hours results in a fine white precipitate. The product is very poorly soluble in pyridine, chloroform, and dichloromethane, but multinuclear NMR spectroscopy gives no evidence for the pyridine analog of **4**. However, a disparity between expected and observed elemental analysis data for **5** suggests the possibility of impurities analogous to **4** that are too insoluble to observe. The synthesis of **5** is easily performed on a 5 gram scale in 77% yield from two very inexpensive and commercially available reagents, providing trivial access to this diphosphorylation reagent. In the pursuit of a more soluble and spectroscopically pure N-donor base adduct of P_2O_5, we similarly investigated the reaction of $(P_2O_5)_\infty$ with triethylamine, tributylamine, 4-*tert*-butylpyridine, and DMF (dimethylformamide). A rapid reaction was observed in all cases, yielding more soluble products than in the case of DABCO and pyridine (see SI). However, these reactions all produced significant side products, and we chose **5** to explore further phosphorylation chemistry.

Treatment of **5** with DABCO led to rapid formation of a mixture of **3** and **4**. To investigate whether **4** is formed in this reaction or if an insoluble pyridine analog was present in the starting **5**, we also treated **5** with DBU. This reaction resulted in clean formation of the DBU adduct, **6** (Figure 4A). Compound **6** is freely soluble in DCM and contains no significant impurities. However, we observed no reactivity between **6** and simple nucleophiles such as methanol and *O*-phenylenediamine.

Combining a suspension of **5** in DCM with a slight excess of diethylamine yields **7** in less than five minutes (Figure 4A). A simple workup provides the diethylammonium salt of **7**, and we were able to obtain a crystal structure of this compound (Figure 4B). We were also able to prepare **7** by treatment of a mixture of **3** and **4** with diethylamine, although in a lower isolated yield (see SI).

Phosphorylation of alcohols with **5** was less facile. Treatment with an excess of methanol gives rise to the expected dimethyl pyrophosphate compound, **8**, as well as a trifunc-

tionalized tetraphosphate derivative **9** (Figure 4A). The corresponding diethylamino derivative of **9** was also observed as a minor impurity in the crude reaction of **5** with diethylamine, but this impurity was easily removed due to poor solubility in cold acetonitrile. However, we were unable to develop conditions for purification of **8** from **9**. Treatment of **5** with more sterically demanding alcohols such as neopentanol and adenosine yielded only complex mixtures of products.

Compound **5** reacts rapidly with phosphate nucleophiles, and treatment with the TBA salt of adenosine monophosphate (AMP) leads to adenosine-substituted TriMP (**10**) in less than five minutes with only minor impurities observed in the $^{31}P\{^{1}H\}$ NMR spectrum. This transformation is reminiscent of the Khorana[7] and Ludwig-Eckstein[23] reactions which append pyrophosphate to form a nucleoside substituted TriMP intermediate. However, the present reaction is markedly cleaner and more selective than those canonical reactions, whose difficult chromatographic separations have spawned decades of research.[6] Additionally, this reactivity of neutral doubly zwitterionic **5** is in stark contrast to the slow reaction of the dianonic imidazole adduct of P_2O_5 with AMP to form diadenosine tetraphosphate.[17]

Intermediate **10** is the same compound observed in Taylor[13] and Jessen's[3,14] syntheses of NTPs and is therefore amenable to a variety of ring opening reactions, which were briefly investigated in one-pot procedures starting from **5**. Treatment of **10** with water results in ring opening to ATP in seconds; the ATP was purified by anion exchange HPLC (AX-HPLC) yielding the ammonium salt of ATP(**11**, Figure 4B). Similarly, treatment of **10** with diethylamine resulted in γ-diethylamino-ATP, which was purified by AX-HPLC (**12**, Figure 4B). Additionally, **10** can be ring opened by treatment with UMP in the presence of $MgCl_2$. This results in selective formation of adenosine uridine tetraphosphate (**13**) isolated as its ammonium salt after purification by AX-HPLC. A number of syntheses of dinucleoside tetraphosphates have been reported,[24] and this synthesis, as well as Wright's[17] are convenient due to their high yields and utilization of NMP substrates rather than more expensive and difficult to synthesize NTPs. Furthermore, the present synthesis provides convenient access to unsymmetrical dinucleoside tetraphosphates, which is not possible with Wright's reagent. Lastly, longer nucleoside oligophosphates are competent phosphorylation substrates, albeit with reduced yield, and treatment of **5** with the TBA salt of ADP and subsequent hydrolysis yields adenosine tetraphosphate (**14**).

Acknowledgement We thank Dr. Peter Müller for help collecting X-ray crystal data. Research reported in this publication was supported by the National Institutes of Health under award number R01GM130936.

Supporting Information Available

See the supporting information for experimental details, further characterization data, and X-ray crystallographic information.

X-ray crystallographic data for C49H53N2O11P5S (CCDC 2004821)

X-ray crystallographic data for C12H24N4O5P2 (CCDC 2071686)

X-ray crystallographic data for C22.50H46.50N7O10P4 (CCDC 2059218)

X-ray crystallographic data for C16H44N4O5P2 (CCDC 2071687)

References

(1) Shepard, S. M.; Cummins, C. C. Functionalization of intact trimetaphosphate: a triphosphorylating reagent for C, N, and O nucleophiles. *J. Am. Chem. Soc.* **2019**, *141*, 1852–1856.

(2) Shepard, S. M.; Windsor, I. W.; Raines, R. T.; Cummins, C. C. Nucleoside Tetra-and Pentaphosphates Prepared Using a Tetraphosphorylation Reagent Are Potent Inhibitors of Ribonuclease A. *J. Am. Chem. Soc.* **2019**, *141*, 18400–18404.

(3) Singh, J.; Steck, N.; De, D.; Hofer, A.; Ripp, A.; Captain, I.; Keller, M.; Wender, P. A.; Bhandari, R.; Jessen, H. J. A phosphoramidite analogue of cyclotriphosphate enables iterative polyphosphorylations. *Angew.Chem., Int. Ed.* **2019**, *131*, 3968–3973.

(4) Mohamady, S.; Desoky, A.; Taylor, S. D. Sulfonyl imidazolium salts as reagents for the rapid and efficient synthesis of nucleoside polyphosphates and their conjugates. *Org. Lett.* **2012**, *14*, 402–405.

(5) Knouse, K. W.; Justine, N.; Schmidt, M. A.; Zheng, B.; Vantourout, J. C.; Kingston, C.; Mercer, S. E.; Mcdonald, I. M.; Olson, R. E.; Zhu, Y., et al. Unlocking P (V): Reagents for chiral phosphorothioate synthesis. *Science* **2018**, *361*, 1234–1238.

(6) Liao, J.-Y.; Bala, S.; Ngor, A. K.; Yik, E. J.; Chaput, J. C. P (V) Reagents for the Scalable Synthesis of Natural and Modified Nucleoside Triphosphates. *J. Am. Chem. Soc.* **2019**, *141*, 13286–13289.

(7) Khorana, H. Carbodiimides. Part V. 1 A Novel Synthesis of Adenosine Di-and Triphosphate and P1, P2-Diadenosine-5'-pyrophosphate. *J. Am. Chem. Soc.* **1954**, *76*, 3517–3522.

(8) R Kore, A.; Srinivasan, B. Recent advances in the syntheses of nucleoside triphosphates. *Curr. Org. Synth.* **2013**, *10*, 903–934.

(9) Bezold, D.; Dürr, T.; Singh, J.; Jessen, H. J. Cyclotriphosphate: A Brief History, Recent Developments, and Perspectives in Synthesis. *Chem. - Eur. J.* **2019**,

(10) Mohamady, S.; Taylor, S. D. Synthesis of nucleoside tetraphosphates and dinucleoside pentaphosphates via activation of cyclic trimetaphosphate. *Org. Lett.* **2013**, *15*, 2612–2615.

(11) Mohamady, S.; Taylor, S. D. Synthesis of nucleoside 5'-tetraphosphates containing terminal fluorescent labels via activated cyclic trimetaphosphate. *J. Org. Chem.* **2014**, *79*, 2308–2313.

(12) Mohamady, S.; Taylor, S. D. One flask synthesis of 2', 3'-cyclic nucleoside monophosphates from unprotected nucleosides using activated cyclic trimetaphosphate. *Tetrahedron Lett.* **2016**, *57*, 5457–5459.

(13) Mohamady, S.; Taylor, S. D. Synthesis of nucleoside triphosphates from 2'-3'-protected nucleosides using trimetaphosphate. *Org. Lett.* **2016**, *18*, 580–583.

(14) Singh, J.; Ripp, A.; Haas, T. M.; Qiu, D.; Keller, M.; Wender, P. A.; Siegel, J. S.; Baldridge, K. K.; Jessen, H. J. Synthesis of Modified Nucleoside Oligophosphates Simplified: Fast, Pure, and Protecting Group Free. *J. Am. Chem. Soc.* **2019**, *141*, 15013–15017.

(15) Jiang, Y.; Chakarawet, K.; Kohout, A. L.; Nava, M.; Marino, N.; Cummins, C. C. Dihydrogen Tetrametaphosphate,[P4O12H2] 2– : Synthesis, Solubilization in Organic Media, Preparation of its Anhydride [P4O11] 2–and Acidic Methyl Ester, and Conversion to Tetrametaphosphate Metal Complexes via Protonolysis. *J. Am. Chem. Soc.* **2014**, *136*, 11894–11897.

(16) Shepard, S. M.; Kim, H.; Bang, Q. X.; Alhokbany, N.; Cummins, C. C. Synthesis of α, δ-Disubstituted Tetraphosphates and Terminally-Functionalized Nucleoside Pentaphosphates. *J. Am. Chem. Soc.* **2020**,

(17) Yanachkov, I. B.; Dix, E. J.; Yanachkova, M. I.; Wright, G. E. P 1, P 2-diimidazolyl derivatives of pyrophosphate and bisphosphonates–synthesis, properties, and use in preparation of dinucleoside tetraphosphates and analogs. *Org. Biomol. Chem.* **2011**, *9*, 730–738.

(18) Meisel, M.; Bock, H.; Solouki, B.; Kremer, M. Erzeugung und Ionisationsmuster der iso (valenz) elektronischen Verbindungen $ClP(=O)_2$ und $ClP(=S)_2$. *Angew. Chem.* **1989**, *101*, 1378–1381.

(19) Pyykkö, P. Additive covalent radii for single-, double-, and triple-bonded molecules and tetrahedrally bonded crystals: a summary. *J. Phys. Chem. A* **2015**, *119*, 2326–2337.

(20) Ramirez, F.; Marecek, J. F. Amine catalysis in phosphoryl transfer from 2, 4-dinitrophenyl phosphate in aprotic and protic solvents. *Tetrahedron* **1979**, *35*, 1581–1589.

(21) Yanachkov, I.; Wright, G. E. Reactive pyrophosphoric and bisphosphonic acid derivatives and methods of their use. 2012; US Patent 8,288,545.

(22) Stachel, D.; Svoboda, I.; Fuess, H. Phosphorus pentoxide at 233 K. *Acta Crystallogr., Sect. C: Struct. Chem.* **1995**, *51*, 1049–1050.

(23) Ludwig, J.; Eckstein, F. Rapid and efficient synthesis of nucleoside 5'-0-(1-thiotriphosphates), 5'-triphosphates and 2', 3'-cyclophosphorothioates using 2-chloro-4H-1, 3, 2-

benzodioxaphosphorin-4-one. *J. Org. Chem.* **1989**, *54*, 631–635.
(24) Appy, L.; Chardet, C.; Peyrottes, S.; Roy, B. Synthetic Strategies for Dinucleotides Synthesis. *Molecules* **2019**, *24*, 4334.

Graphical TOC Entry

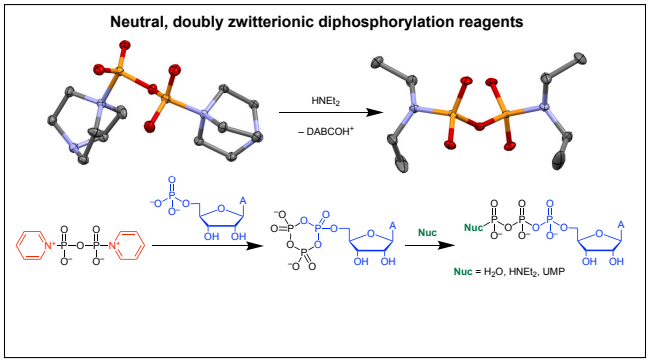

N-donor Base Adducts of P_2O_5 as Diphosphorylation Reagents

Scott M. Shepard[1] and Christopher C. Cummins[1,2]

[1]Department of Chemistry, Massachusetts Institute of Technology, Cambridge MA
[2]ccummins@mit.edu

Contents

1 General Considerations

All chemical syntheses were performed in a Vacuum Atmospheres model MO-40M glovebox under an inert atmosphere of purified nitrogen unless otherwise stated. All solvents used in the glovebox were obtained anhydrous and oxygen-free by bubble degassing with argon and purification through columns of alumina and Q5 by the method of Grubbs, except for water and acetone.[1] HPLC grade water was purchased from Sigma Aldrich and used as received. Dried acetone was prepared by stirring overnight over anhydrous calcium sulfate followed by distillation under an anhydrous nitrogen atmosphere from fresh calcium sulfate.[2] The tetrabutylammonium (TBA) salts of 5'-UMP, 5'-AMP, and 5'-ADP were prepared according to the procedure of Taylor,[3] by ion exchange on Dowex 50WX8 (H+) followed by neutralization with TBA hydroxide and subsequent lyophilization. The resulting TBA nucleotide salts were stored as either DMF or acetonitrile stock solutions (0.10 g/mL) over 4Å molecular sieves (dried under vacuum at 200 °C for 24 hours) for at least 24 hours prior to use. $[PPN]_3[P_3O_9] \cdot (H_2O)$[4] was prepared according to the literature procedure. All other reagents were purchased and used as received. Deuterated solvents were purchased from Cambridge Isotope Labs and used as received. NMR spectra were obtained at ambient temperature (ca. 25 °C) on a Bruker Avance 400 instrument. ^{1}H and ^{13}C NMR spectra were referenced internally to residual solvent signals. ^{31}P NMR spectra were referenced internally to the PPN signal or externally to 85% phosphoric acid. Electrospray ionization mass spectra (ESI-MS(−)) were acquired on a Micromass Q-TOF ESI spectrometer. Samples were prepared in acetonitrile or acetonitrile/water at an approximate concentration of 20 ng/μL, and a source temperature of 80 °C and desolvation gas temperature of 400 °C were used. Elemental analyses were performed by Midwest Microlab. HPLC was performed with Waters 515 HPLC pumps coupled to a Waters 2487 UV absorbance detector and a PRP-X100 anion exchange column. HPLC purifications were carried out with a gradient method from 100% A, 0% B to 0% A, 100% B (A = 100% water; B = 1M $(NH_4)(HCO_3)$ in water) with a 2.5 mL/min flow rate. The HPLC purifications were monitored by absorbance at 260 nm.

2 Synthesis and Characterization of Compounds

2.1 Synthesis of [PPN][HNEt$_3$][1]

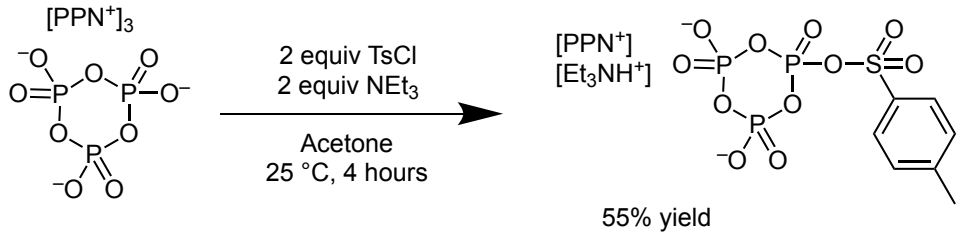

Figure S1: Synthesis of [PPN][HNEt$_3$][**1**].

In a glovebox, $[PPN]_3[P_3O_9]\cdot(H_2O)^4$ (1.36 g, 0.72 mmol) was suspended in 10 mL of anhydrous acetone. (Note: At a concentration less than 1 g/mL, precipitation does not occur in the following step.) To this stirring suspension was added triethylamine (0.20 mL, 1.43 mmol) followed by a solution of TsCl (0.27 g, 1.43 mmol) in anhydrous acetone (2 mL). The solution was stirred vigorously for 15 min. After the addition of reagents, the mixture briefly became homogeneous before a thick precipitate formed. The mixture was then filtered through Celite® to remove the precipitate. The resulting colorless solution was left undisturbed at ambient temperature for 12 hours, resulting in precipitation of colorless crystals. The supernatant solution was decanted off the crystals, which were then rinsed three times with 1 mL of acetone. The resulting crystals were dried under vacuum, yielding the product as a white, crystalline solid (0.41 g, 0.39 mmol, 55% yield). The product was stored in the glovebox freezer at −35 °C to prevent decomposition.

Elem. Anal. Found(Calc'd) for $C_{49}H_{53}N_2O_{11}P_5S$: C 56.35 (56.98), H 6.88 (5.17), N 3.29 (2.71). We had difficulty obtaining satisfactory EA data for this salt of **1**, perhaps due to the fact that the compound decomposes readily at room temperature.

^{1}H NMR (acetonitrile-d_3, 400 MHz): δ 10.07 (br, 1H), 7.96 (d, J = 8.1 Hz, 2H), 7.79 to 7.35 (m, 60H), 7.14 (d, J = 7.8 Hz, 2H), 3.06 (dt, J = 11.9, 6.1 Hz, 6H), 2.44 (s, 3H), 1.22 (t, J = 7.3 Hz, 9H).

^{13}C{^{1}H} NMR (acetonitrile-d_3, 100.6 MHz): δ 134.54, 133.83 to 132.72 (m), 131.01 to 130.08 (m), 128.68 (d, J = 2.1 Hz), 127.60 (d, J = 2.0 Hz), 126.59 (d, J = 1.7 Hz), 47.07, 30.83, 21.21, 8.96.

^{31}P{^{1}H} NMR (acetonitrile-d_3, 162.0 MHz): δ 23.01, −21.94 (d, J = 25.3 Hz), −32.54 (t, J = 25.7 Hz).

ESI-MS(−) of $[C_7H_7O_{11}P_3S]H^-$ (CH_3CN, m/z) 392.88 (calc'd 392.90)

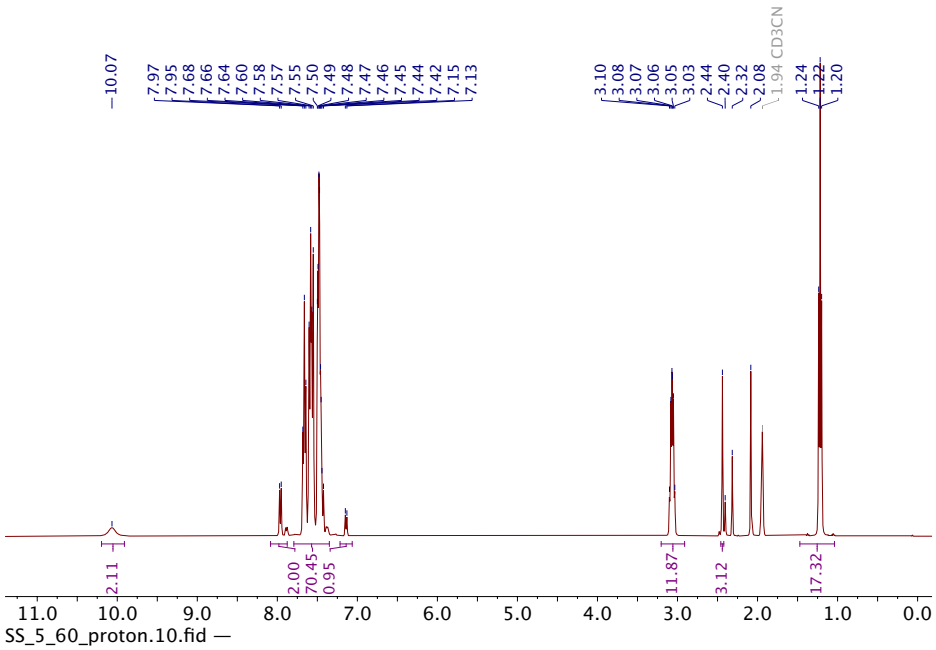

Figure S2: ^{1}H NMR spectrum of [PPN][HNEt$_3$][**1**] (acetonitrile-d_3, 400 MHz).

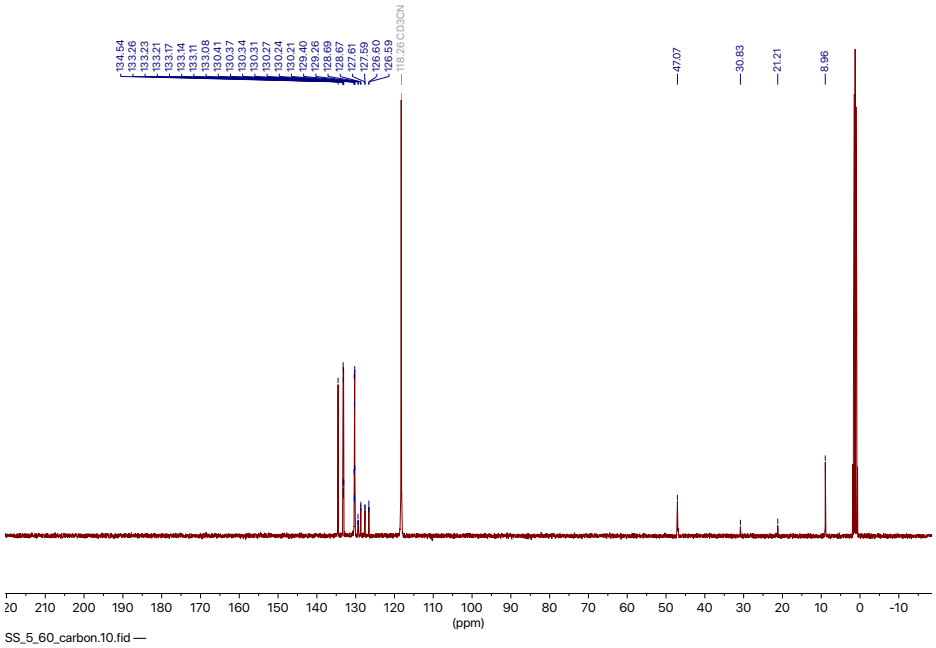

Figure S3: ^{13}C NMR spectrum of [PPN][HNEt$_3$][**1**] (acetonitrile-d_3, 100.6 MHz).

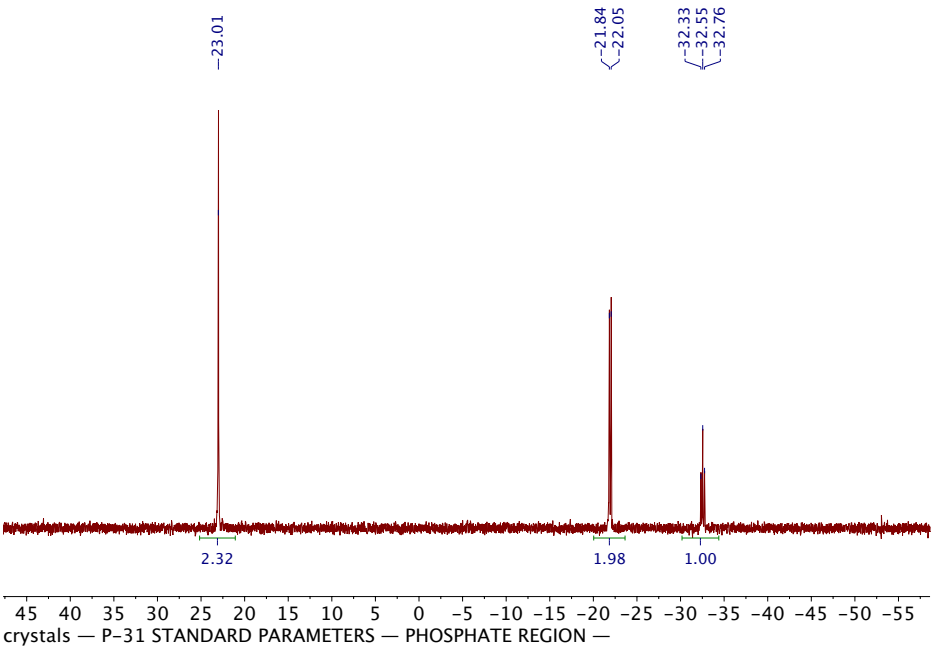

Figure S4: $^{31}P\{^{1}H\}$ NMR spectrum of [PPN][$HNEt_3$][**1**] (acetonitrile-d_3, 162.0 MHz).

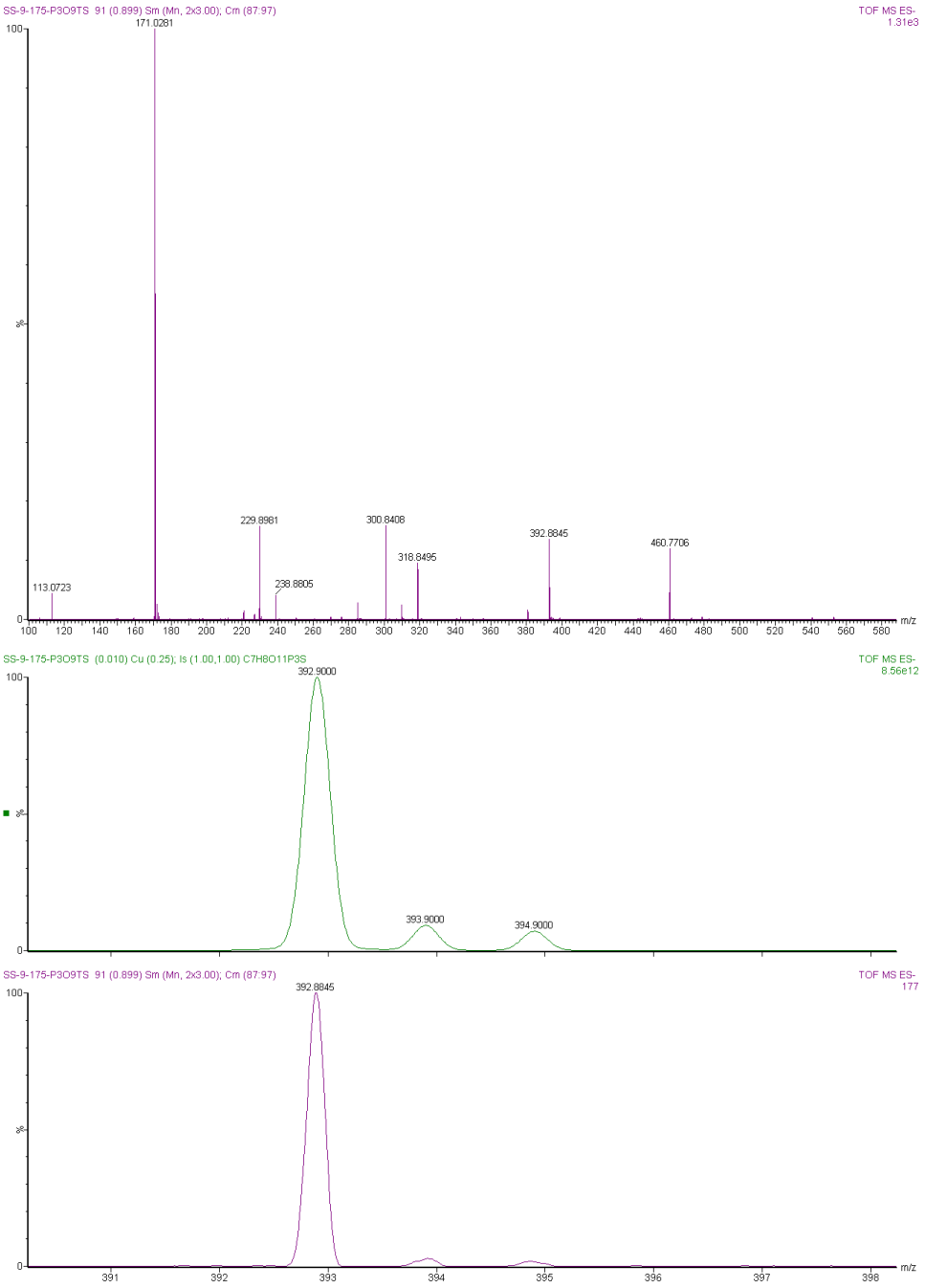

Figure S5: ESI-MS(−) of [PPN][HNEt$_3$][**1**] (CH_3CN) with zoomed in portion showing the molecular ion ([$C_7H_7O_{11}P_3S$]H$^-$, bottom), and calculated isotope pattern (top).

2.2 Treatment of 1 with DABCO to form 2

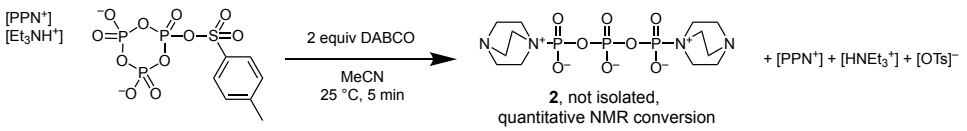

Figure S6: Formation of anion **2**.

In the glovebox, [PPN][$HNEt_3$][**1**] (0.080 g, 0.077 mmol) was dissolved in acetonitrile (2 mL). To this solution was added DABCO (0.018 g, 0.16 mmol) in acetonitrile (1 mL). The solution was briefly mixed, and $^{31}P\{^1H\}$ NMR showed quantitative conversion to anion **2**. Attempts to obtain a solid salt of anion **2**, for example by precipitation with diethyl ether, solvent evaporation, or cooling a concentrated solution to −35 °C resulted in significant decomposition to a complex mixture of phosphates.

$^{31}P\{^1H\}$ NMR (acetonitrile-d_3, 202 MHz): δ) 23.00, −7.03 (d, J = 21.4 Hz), −20.90 (t, J = 21.9 Hz).

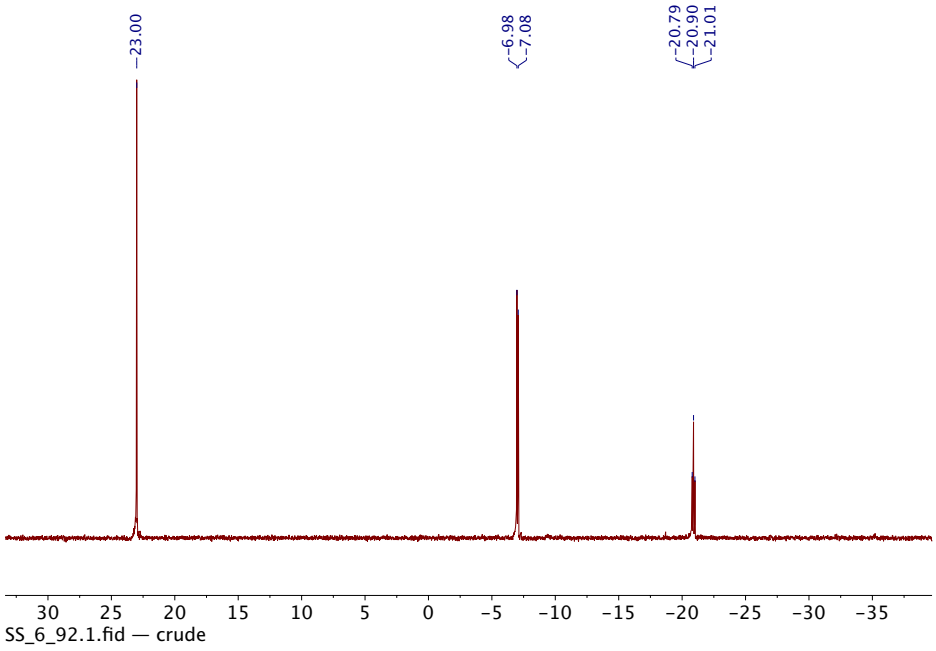

Figure S7: $^{31}P\{^1H\}$ NMR spectrum of the crude reaction mixture containing **2** (acetonitrile-d_3, 202 MHz).

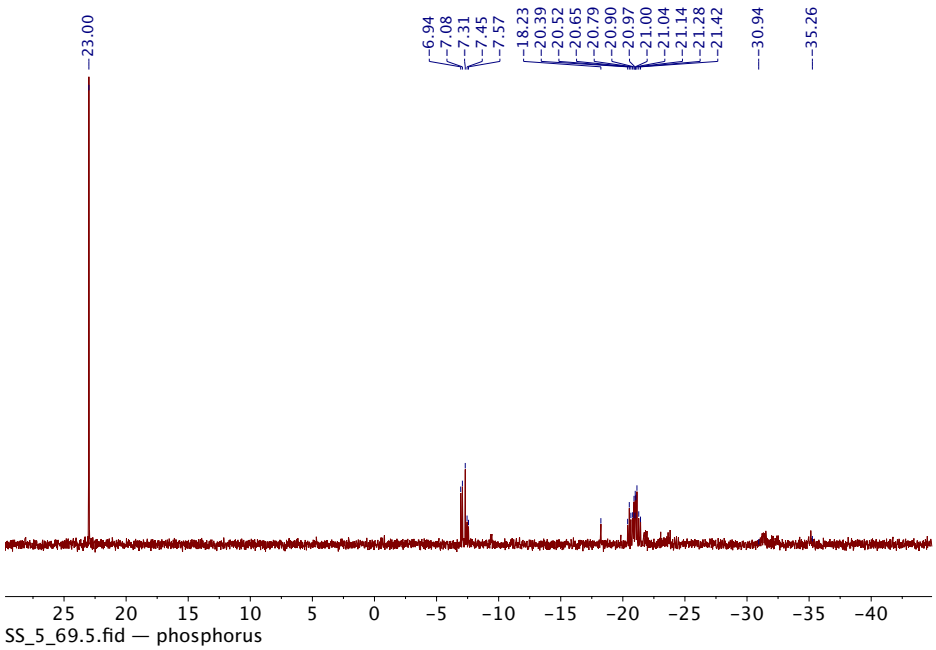

Figure S8: $^{31}P\{^{1}H\}$ NMR spectrum of the solid obtained after precipitating the crude reaction mixture containing **2** with diethyl ether (acetonitrile-d_3, 202 MHz).

2.3 Attempted formation of 2 in one pot from TriMP

The reagents used for the synthesis of **2** from TriMP were combined in one pot rather than proceeding through isolated **1**. This is analogous to the procedure employed by Taylor.[5]

In a glovebox, a stock solution was prepared of $[TBA]_3[P_3O_9]\cdot H_2O$ in acetonitrile at a concentration of 0.10 g/mL. This solution was stored over activated 4Å sieves for at least 24 hours. To this solution of $[TBA]_3[P_3O_9]\cdot H_2O$ (0.50 mL, 0.052 mmol) was added triethylamine (0.015 mL, 0.10 mmol). To this mixture was then added a solution of MstCl (0.011 g, 0.052 mmol) in acetonitrile (0.5 mL) followed by a solution of DABCO (0.023 g, 0.21 mmol) in acetonitrile (0.5 mL). The resulting mixture was mixed and analyzed by $^{31}P\{^{1}H\}$ NMR.

$^{31}P\{^{1}H\}$ NMR analysis reveals a complex mixture of phosphates (Figure S9). Dominant, assignable species are **2** and TriMP. The majority of the other phosphorus environments correspond to two or more species with chemical shifts similar to that of **1**. One of these species may correspond to the Mst analog of **1**. Another possible species is μ-oxo-bis-trimetaphosphate ($[P_3O_8\text{-}O\text{-}P_3O_8]^{4-}$). There are also numerous difficult to assign species with small integrations. While this mixture appears to contain **2**, the numerous other species likely result in side products when this mixture is used for phosphorylation reactions.

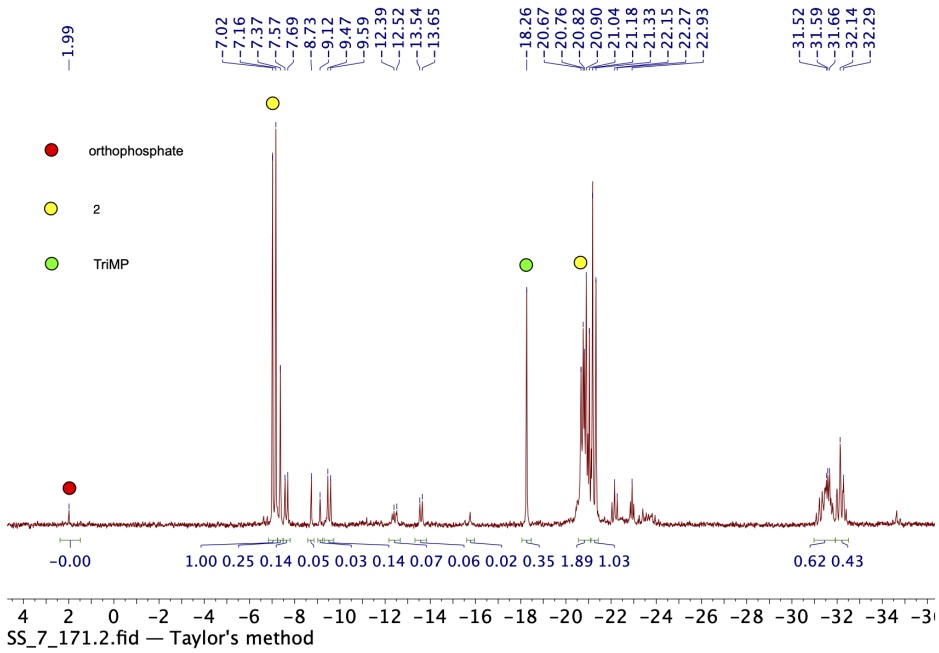

Figure S9: $^{31}P\{^{1}H\}$ NMR (202 MHz, acetonitrile) of the mixture resulting from mixing $[TBA]_3[P_3O_9]\cdot H_2O$, triethylamine, MstCl, and DABCO in acetonitrile as described above.

2.4 Synthesis of 3 and 4

The following three synthetic methods give spectroscopically identical mixtures of **3** and **4**, differing only in the ratio of the two products.

2.4.1 Synthesis of 3 and 4 from 1

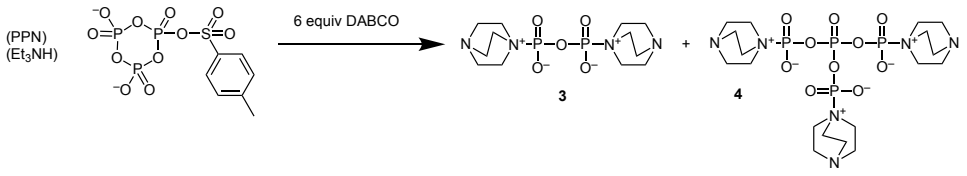

Figure S10: Synthesis of **3** and **4** from **1**.

In the glovebox, [PPN][$HNEt_3$][**1**] (0.75 g, 0.72 mmol) was dissolved in acetonitrile (5 mL). To this solution was added a solution of DABCO (0.49 g, 4.3 mmol) in acetonitrile (5 mL). The resulting solution was allowed to stand overnight, whereupon colorless crystals precipitated. The supernatant solution was then decanted off, and the crystals were rinsed with acetonitrile (3 × 3 mL). The crystals were then dried under vacuum yielding the product, a mixture of **3** and **4** as a white, crystalline solid (0.13 g). Proton NMR integration gives a 1.7:1 ratio of **3** to **4**.

2.4.2 Synthesis of 3 from TriMP

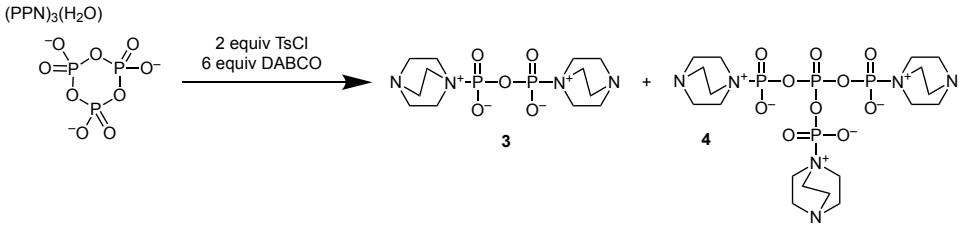

Figure S11: Synthesis of **3** and **4** from TriMP.

In the glovebox, $[PPN]_3[P_3O_9]\cdot(H_2O)$[4] (0.28 g, 0.15 mmol) and DABCO (0.10 g, 0.90 mmol) were dissolved in acetonitrile (5 mL). To this stirring solution was added a solution of TsCl (0.056 g, 0.30 mmol) in acetonitrile (2 mL). The resulting solution was allowed to stand overnight, whereupon colorless crystals precipitated. The supernatant solution was then decanted off, and the crystals were rinsed with acetonitrile (3 × 3 mL). The crystals were then dried under vacuum yielding the product, a mixture of **3** and **4** as a white, crystalline solid (0.048 g). Proton NMR integration gives a 1.4:1 ratio of **3** to **4**.

2.4.3 Synthesis of 3 from $(P_2O_5)_\infty$

In the glovebox, $(P_2O_5)_\infty$ (0.26 g, 1.8 mmol) was suspended in acetonitrile (10 mL). To this stirring suspension was added a solution of DABCO (0.82 g, 7.3 mmol) in acetonitrile (2 mL). The resulting mixture was stirred for 5 min, resulting in dissolution of most of the solid material. The mixture was then filtered through Celite® to remove any insoluble impurities. The clear filtrate was allowed to stand overnight, whereupon colorless crystals precipitated. The supernatant solution was then decanted off, and the crystals were rinsed with acetonitrile (3 × 3 mL). The crystals were then dried under vacuum yielding the product, a mixture of **3** and **4** as a white, crystalline solid (0.65 g). Proton NMR integration gives a 2.3:1 ratio of **3** to **4**.

2.4.4 Characterization data for 3

^{1}H NMR (chloroform-*d*, 400 MHz): δ 3.58 (t, J = 7.8 Hz, 6H), 3.16 (t, J = 7.6 Hz, 6H).
^{13}C{^{1}H} NMR (chloroform-*d*, 100.6 MHz): δ 47.79, 45.27 (d, J = 2.2 Hz).
^{31}P{^{1}H} NMR (chloroform-*d*, 162.0 MHz): δ −11.01.

2.4.5 Characterization data for 4

^{1}H NMR (chloroform-*d*, 400 MHz): δ 3.64 (t, J = 8.6 Hz, 6H), 3.16 (t, J = 8.6 Hz, 6H).
^{13}C{^{1}H} NMR (chloroform-*d*, 100.6 MHz): δ 47.75, 45.20 (d, J = 4.0 Hz).
^{31}P{^{1}H} NMR (chloroform-*d*, 162.0 MHz): δ −11.44 (d, J = 20.6 Hz), −33.85 (q, J = 20.6 Hz).

2.4.6 Spectra of a mixture of 3 and 4

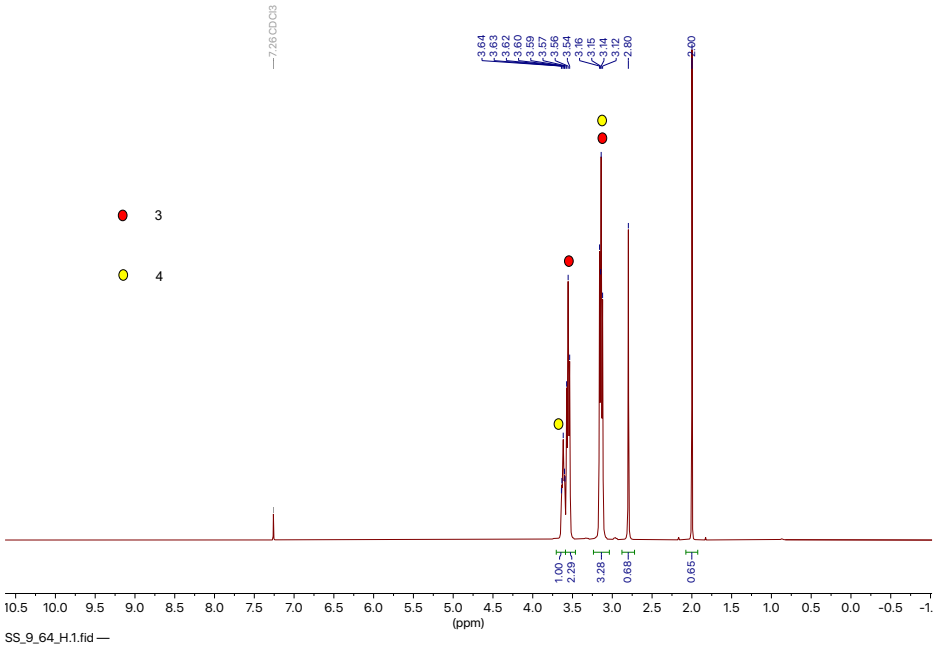

Figure S12: ^{1}H NMR spectrum of a mixture of **3** and **4** (chloroform-*d*, 400 MHz).

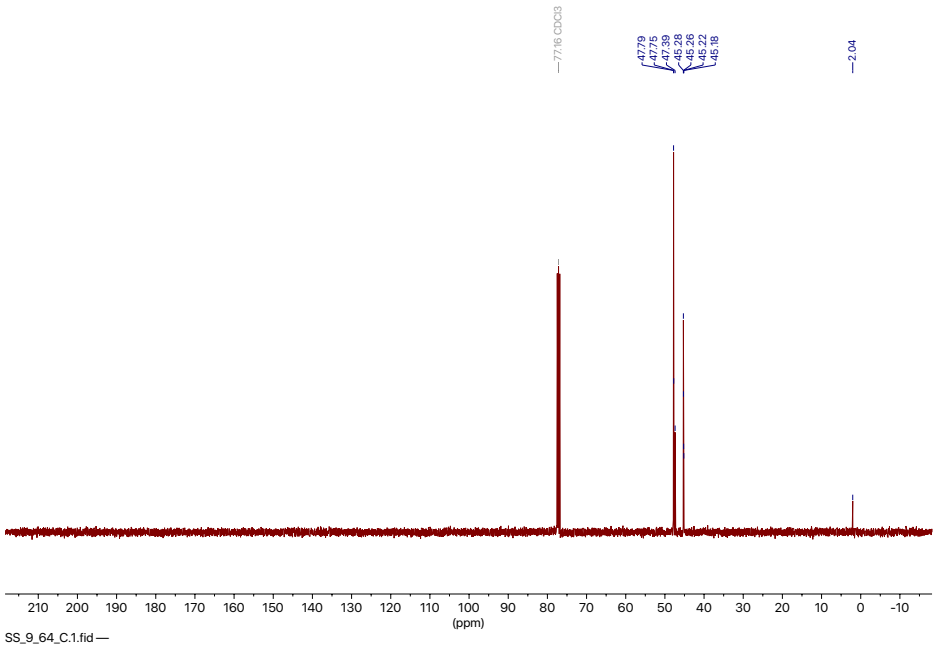

Figure S13: ^{13}C NMR spectrum of a mixture of **3** and **4** (chloroform-*d*, 100.6 MHz).

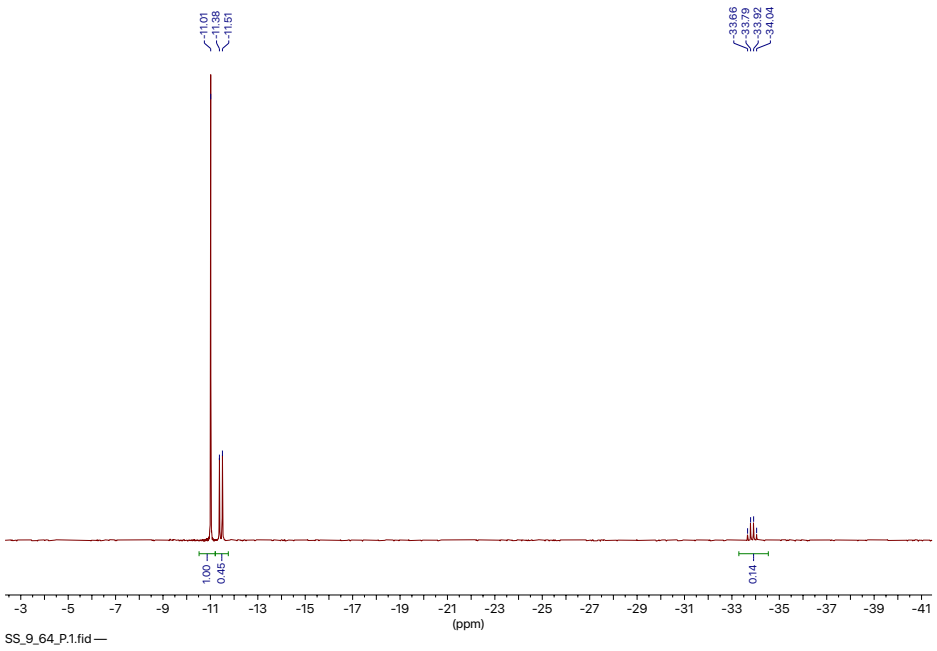

Figure S14: $^{31}P\{^{1}H\}$ NMR spectrum of a mixture of **3** and **4** (chloroform-*d*, 162.0 MHz).

2.5 Synthesis of 5

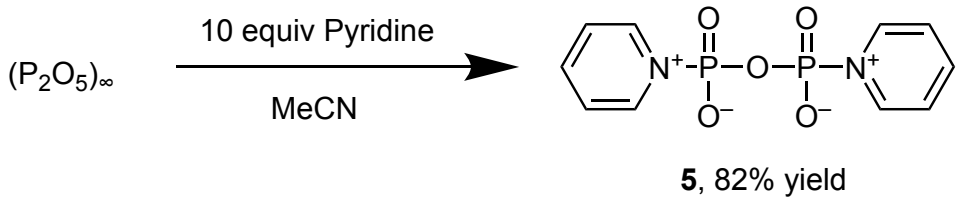

5, 82% yield

Figure S15: Synthesis of **5**.

In the glovebox, a Schlenk tube was charged with $(P_2O_5)_\infty$ (0.19 g, 1.4 mmol) and acetonitrile (10 mL). To this suspension was then added pyridine (1.1 mL, 14 mmol). The vessel was then sealed and removed from the glovebox. The vessel was then placed in an oil bath and the mixture stirred at 70 °C overnight. The vessel was then cooled to room temperature and returned to the glovebox. The fine white precipitate was collected by filtration and rinsed thoroughly with acetonitrile. Drying the solid under vacuum yielded the product as a free flowing white powder (0.36 g, 1.1 mmol, 82% yield). The resulting product is poorly soluble in dichloromethane, chloroform, and pyridine (approximately 1 to 5 mg/mL) and not appreciably soluble in acetonitrile. Heating this material to 180 °C under vacuum results in no change. Heating the material under a methane flame in a glass tube sealed under vacuum result in an insoluble orange/black material.

Elem. Anal. Found(Calc'd) for $C_{10}H_{10}N_2O_5P_2$: C 37.84 (39.02), H 3.38 (3.36), N 9.15 (9.33).

^{1}H NMR (chloroform-*d*, 400 MHz): δ 9.51 (m, 2H), 8.63 to 8.29 (m, 1H), 7.95 (t, J = 7.0 Hz, 2H).

^{13}C{^{1}H} NMR (chloroform-*d*, 100.6 MHz): δ 146.05 (d, J = 23.5 Hz), 136.07, 126.42.

^{31}P{^{1}H} NMR (chloroform-*d*, 162.0 MHz): δ −18.74.

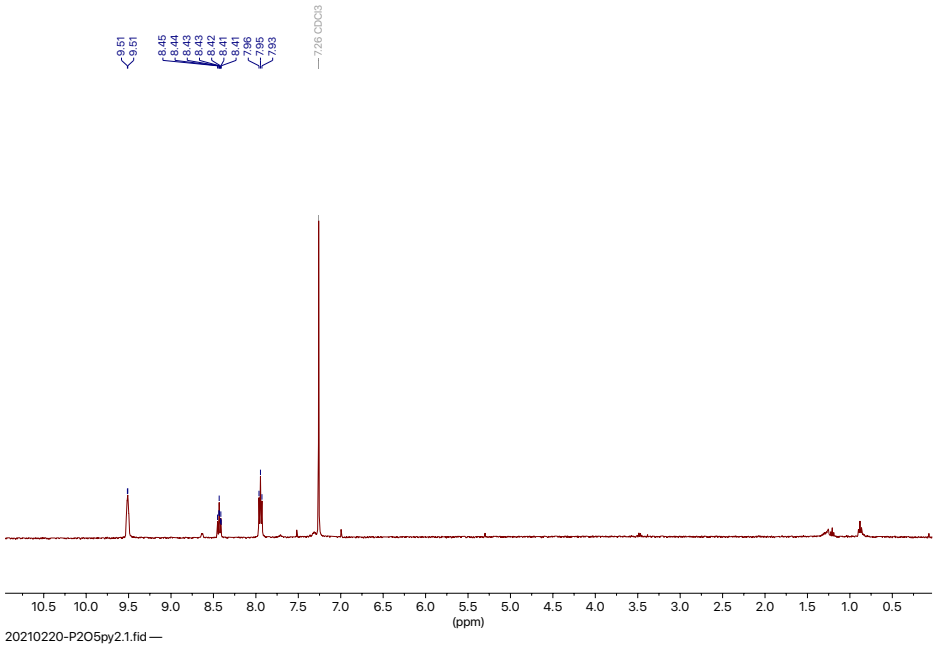

Figure S16: ^{1}H NMR spectrum of **5** (chloroform-*d*, 400 MHz).

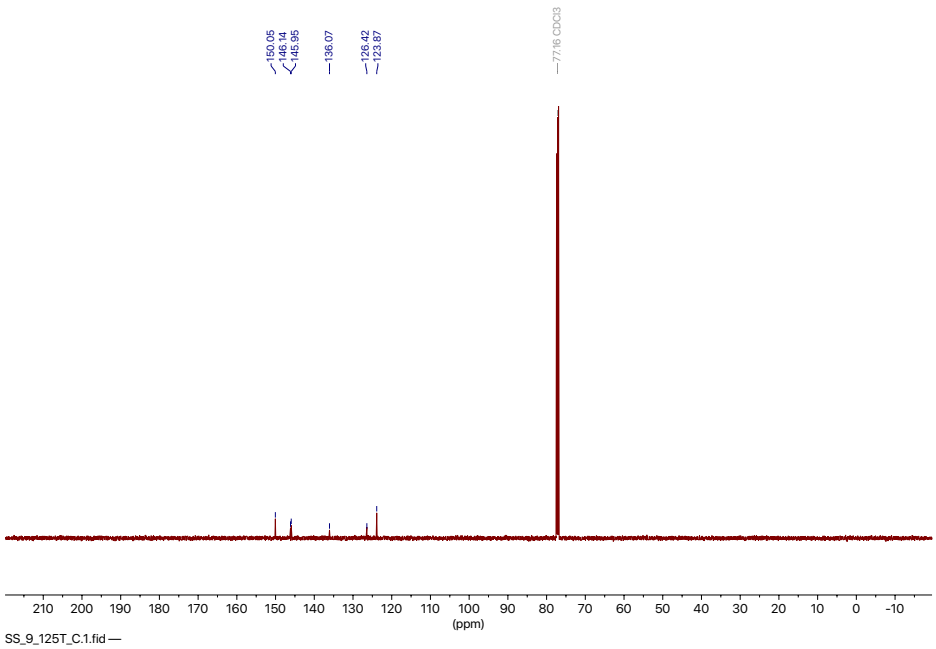

Figure S17: ^{13}C NMR spectrum of **5** (chloroform-*d*, 100.6 MHz).

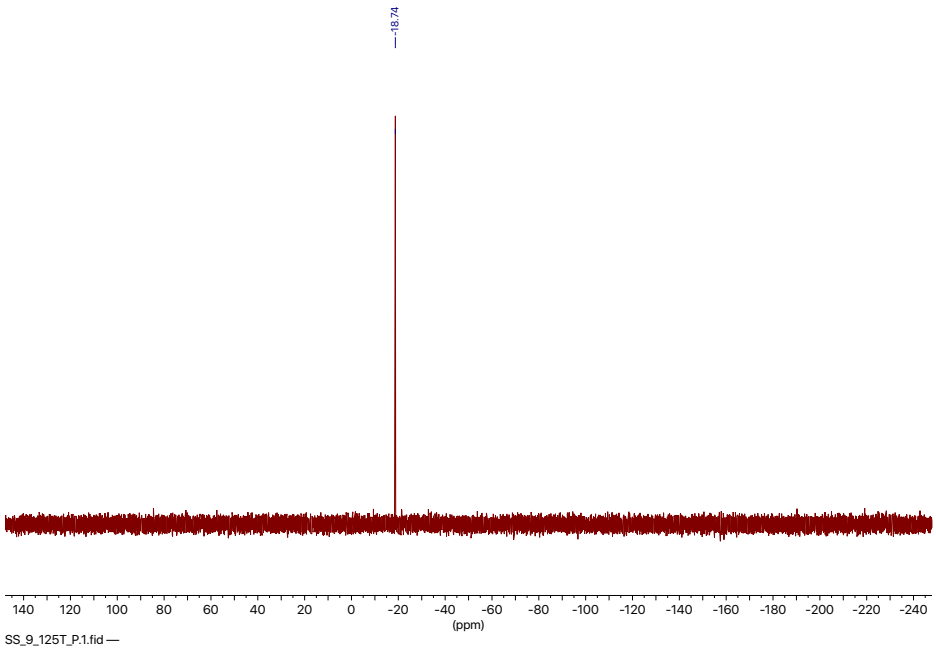

Figure S18: ^{31}P{^{1}H} NMR spectrum of **5** (chloroform-*d*, 162.0 MHz).

2.6 Treatment of $(P_2O_5)_\infty$ with Various N-donor Bases

In a general experiment, $(P_2O_5)_\infty$ (0.050 g, 0.35 mmol) was suspended in acetonitrile (5 mL), in the glovebox. To this stirring suspension was added a solution of an N-donor base (1.4 mmol) in acetonitrile (2 mL) and the resulting mixture stirred for 5 min. During this time, most of the suspended material dissolved. The resulting solution was then analyzed by $^{31}P\{^1H\}$ NMR. The N-donor bases tested were triethylamine, 4-*tert*-butylpyridine, tributylamine, and dimethylformamide.

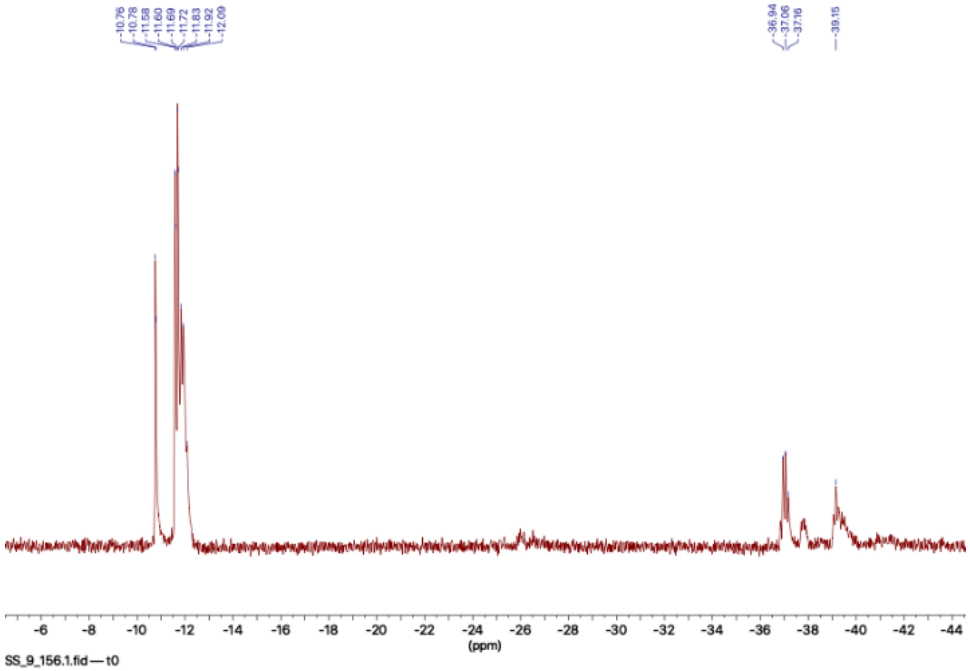

Figure S19: $^{31}P\{^1H\}$ NMR spectrum of reaction mixture resulting from mixing $(P_2O_5)_\infty$ with triethylamine (acetonitrile, 162.0 MHz).

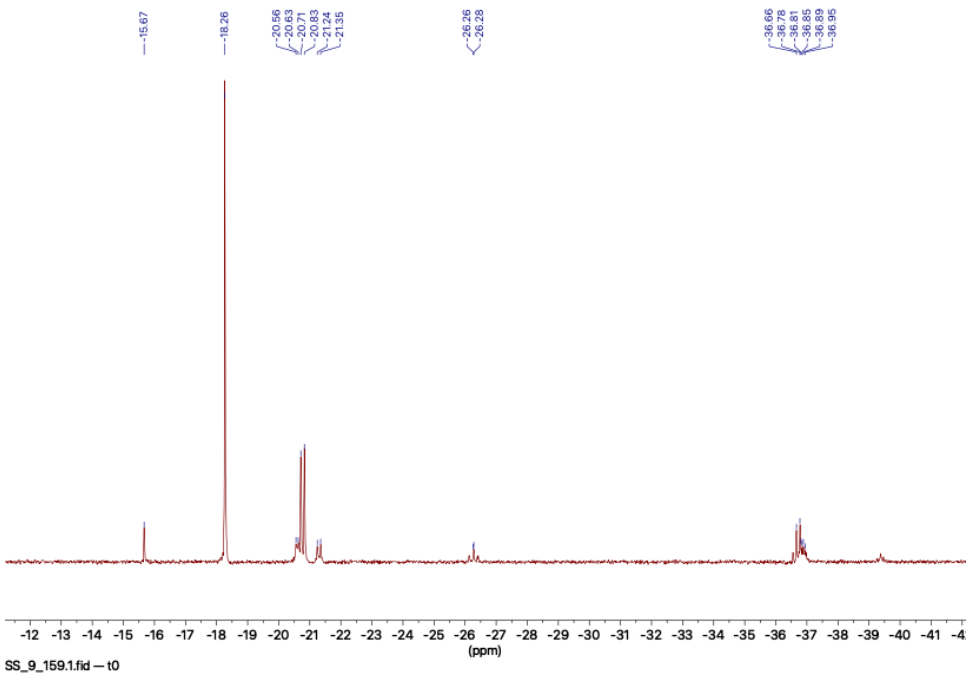

Figure S20: $^{31}P\{^{1}H\}$ NMR spectrum of reaction mixture resulting from mixing $(P_2O_5)_\infty$ with 4-*tert*-butylpyridine (acetonitrile, 162.0 MHz).

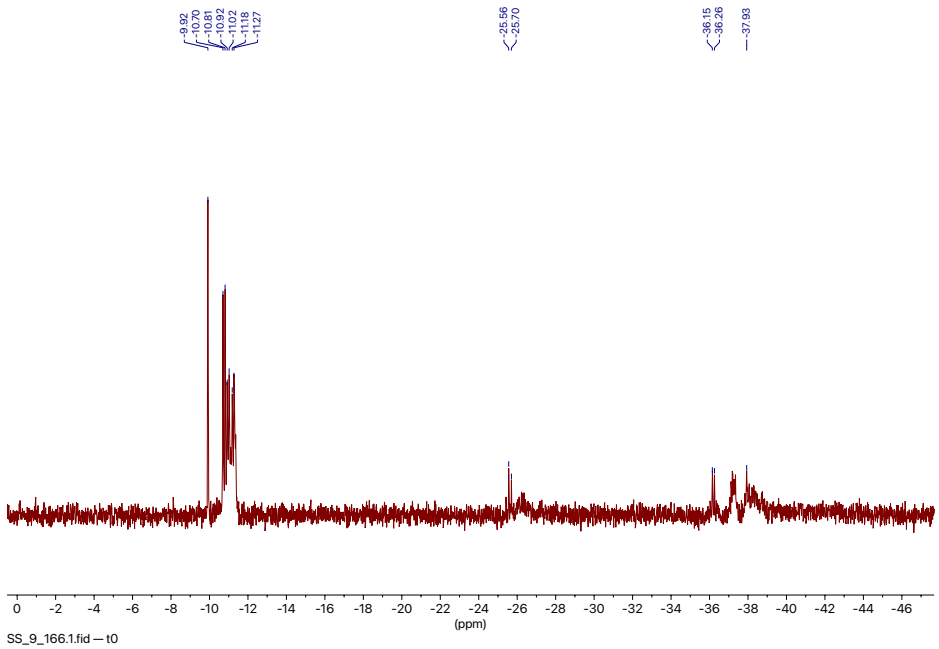

Figure S21: $^{31}P\{^{1}H\}$ NMR spectrum of reaction mixture resulting from mixing $(P_2O_5)_\infty$ with tributylamine (acetonitrile, 162.0 MHz).

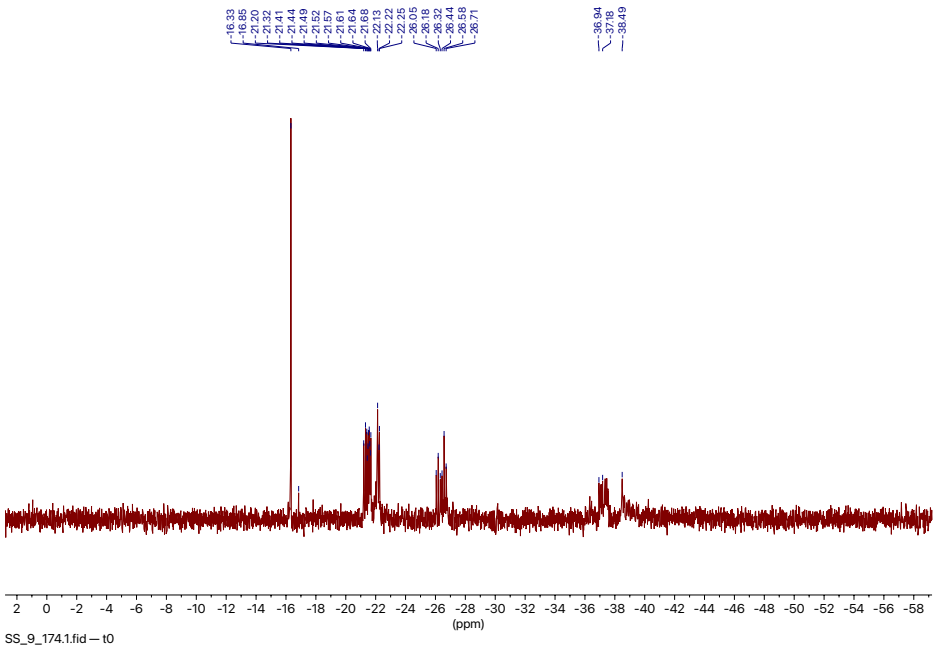

Figure S22: $^{31}P\{^{1}H\}$ NMR spectrum of reaction mixture resulting from mixing $(P_2O_5)_\infty$ with dimethylformamide (acetonitrile, 162.0 MHz).

2.7 Synthesis of 6

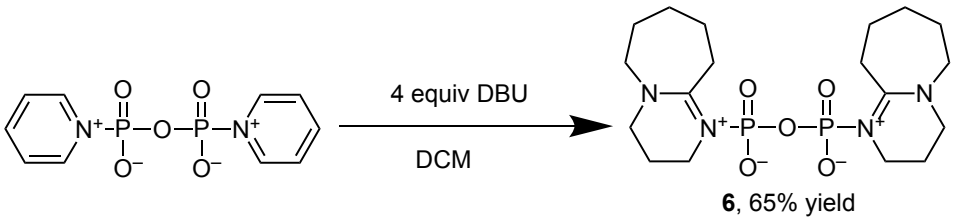

Figure S23: Synthesis of **6**.

In the glovebox, **5** (0.11 g, 0.36 mmol) was suspended in dichloromethane (4 mL). To this stirring suspension was added DBU (0.22 g, 1.5 mmol) in dichloromethane (2 mL). The resulting suspension was stirred for 30 min, resulting in dissolution of most of the solid material. The resulting mixture was filtered through Celite® to remove insoluble material. All volatile materials were then evaporated under reduced pressure, leaving a pale yellow solid. The solid residue was then dissolved in acetonitrile (2 mL) and diethyl ether (15 ml) was added, resulting in a cloudy suspension. The next day, the mixture had settled into a polycrystalline solid. The supernatant was decanted off the crystals, and the solids were rinsed with diethyl ether. The resulting solid was dried under vacuum, giving the product as a white powder (0.10 g, 0.23 mmol, 65% yield).

^{1}H NMR (chloroform-*d*, 400 MHz): δ 3.93 (t, J = 5.4 Hz, 2H), 3.61 to 3.45 (m, 2H), 3.39

(t, J = 6.2 Hz, 2H), 2.07 (p, J = 6.0 Hz, 2H), 1.90 (p, J = 5.8 Hz, 2H), 1.73 (p, J = 5.6 Hz, 2H), 1.69 to 1.60 (m, 2H).

$^{13}C\{^1H\}$ NMR (chloroform-d, 100.6 MHz): δ 170.92 (t, J = 4.4 Hz), 55.23, 50.42, 45.17, 31.39, 28.79, 25.76, 23.02, 20.28 (d, J = 2.1 Hz).

$^{31}P\{^1H\}$ NMR (chloroform-d, 162.0 MHz): δ −15.77.

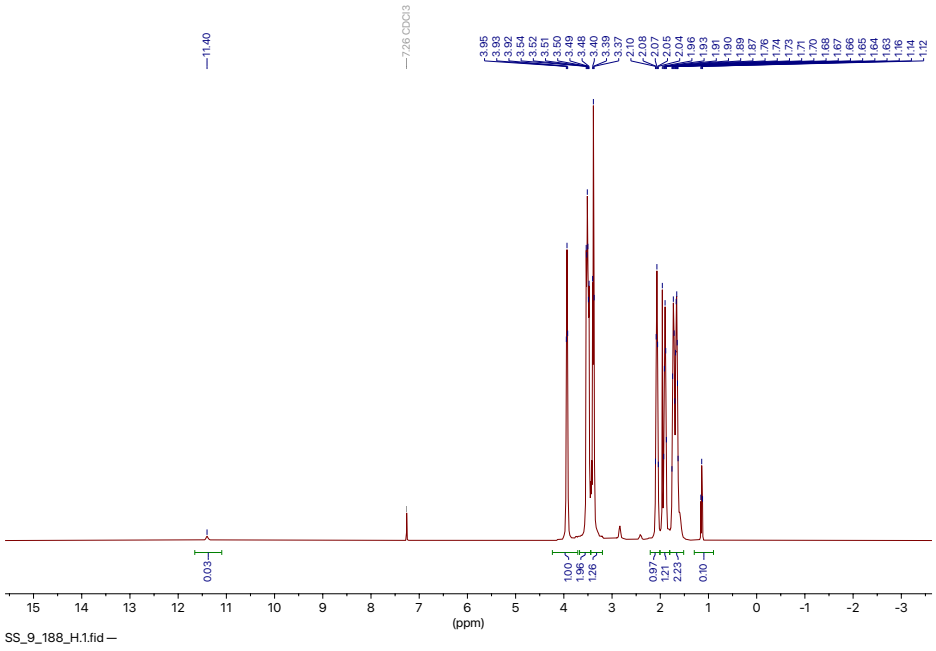

Figure S24: ^{1}H NMR spectrum of **6** (chloroform-d, 400 MHz).

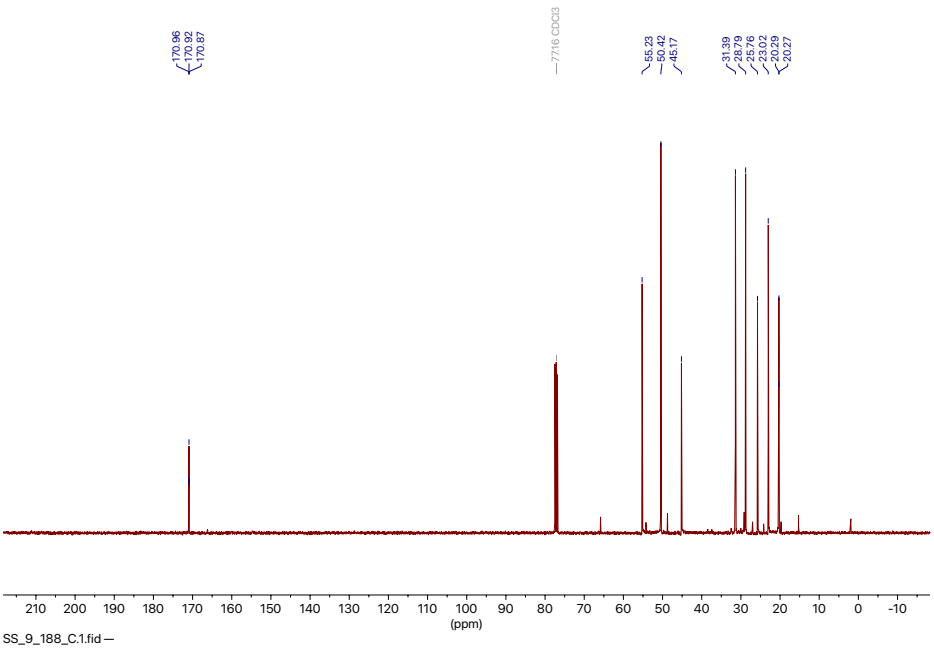

Figure S25: ^{13}C NMR spectrum of **6** (chloroform-*d*, 100.6 MHz).

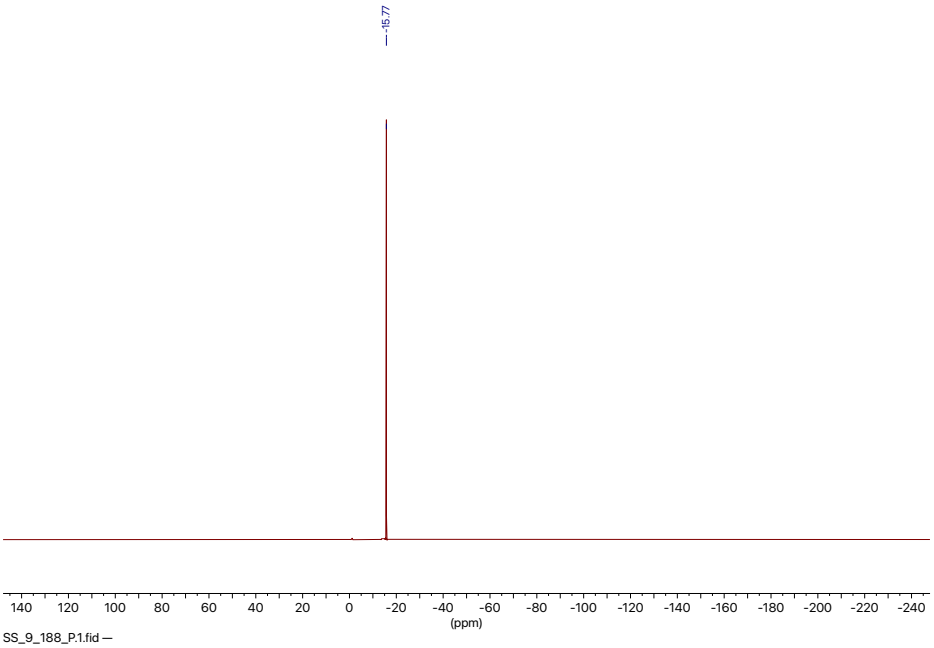

Figure S26: ^{31}P{^{1}H} NMR spectrum of **6** (chloroform-*d*, 162.0 MHz).

2.8 Synthesis of $[H_2NEt_2]_2$[7]

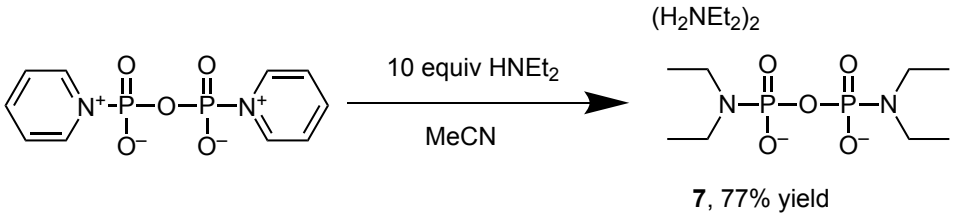

Figure S27: Synthesis of $[H_2NEt_2]_2$[**7**].

Treatment of either a mixture of **3** and **4** or **5** with diethylamine leads immediately to **7** which is purified with a simple workup.

2.8.1 Synthesis of $[H_2NEt_2]_2$[7] from a mixture of 3 and 4

In the glovebox, a mixture of **3** and **4** (0.051 g, a 2.3:1 ratio of **3** to **4** gives 0.098 mmol of **3**) was suspended in dichloromethane (2 mL). To this stirring suspension was added diethylamine (0.10 g, 1.4 mmol) in dichloromethane (2 mL). The resulting suspension was stirred for 5 min, resulting in dissolution of all the starting material. All volatile materials were then evaporated under reduced pressure, leaving a waxy, yellow solid. Rinsing this solid material with cold acetonitrile (3 × 3 mL) removed soluble impurities, leaving a white solid. The resulting solid was dried under vacuum, giving the product as a white powder (0.035 g, 0.068 mmol, 69% yield relative to **3**).

2.8.2 Synthesis of $[H_2NEt_2]_2$[7] from 5

In the glovebox, **5** (0.16 g, 0.52 mmol) was suspended in dichloromethane (4 mL). To this stirring suspension was added diethylamine (0.23 g, 3.1 mmol) in dichloromethane (2 mL). The resulting suspension was stirred for 5 min, resulting in dissolution of all the starting material. Volatiles were then evaporated under reduced pressure, leaving a waxy, yellow solid. Rinsing this solid material with cold acetonitrile (3 × 3 mL) removed soluble impurities, leaving a white solid. The resulting solid was dried under vacuum, giving the product as a white powder (0.18 g, 0.40 mmol, 77% yield).

2.8.3 Characterization data for $[H_2NEt_2]_2$[7]

Elem. Anal. Found(Calc'd) for $C_{16}H_{44}N_4O_5P_2$: C 44.23 (44.22), H 10.21 (10.30), N 12.89 (12.97).

^{1}H NMR (chloroform-*d*, 400 MHz): δ 10.61 (s, 4H), 3.07 (dq, J = 11.6, 7.0 Hz, 8H), 2.88 (q, J = 7.3 Hz, 8H), 1.35 (t, J = 7.3 Hz, 12H), 1.08 (t, J = 7.1 Hz, 12H).

^{13}C{^{1}H} NMR (chloroform-*d*, 100.6 MHz): δ 40.90, 40.05, 14.40, 11.49.

^{31}P{^{1}H} NMR (chloroform-*d*, 162.0 MHz): δ −1.72.

ESI-MS(−) of $[C_8H_{20}N_2O_5P_2]H^-$ (CH_3CN, m/z) 287.16 (calc'd 287.09)

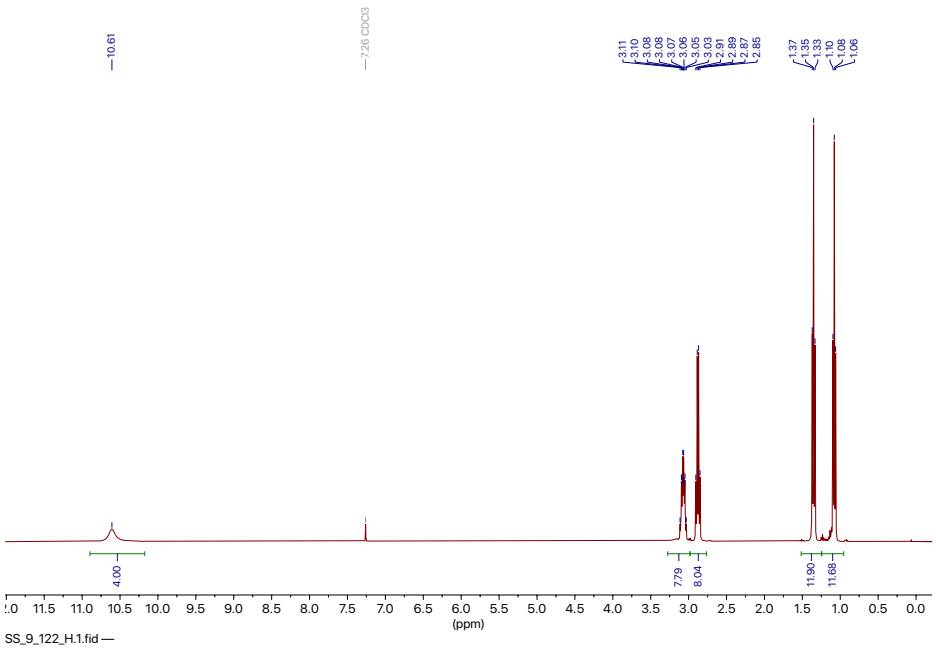

Figure S28: ^{1}H NMR spectrum of $[H_2NEt_2]_2$[**7**] (chloroform-*d*, 400 MHz).

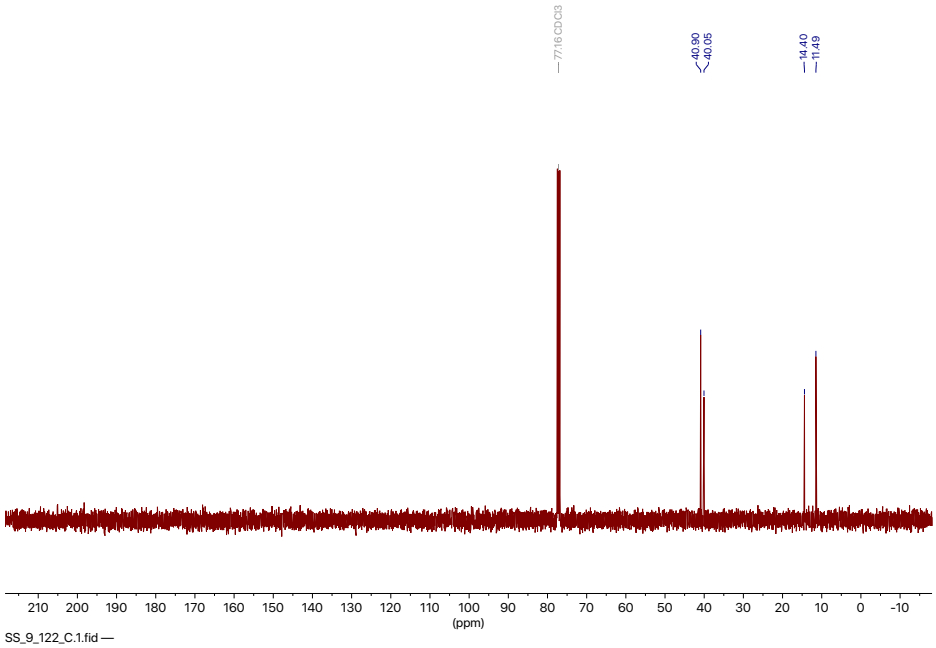

Figure S29: ^{13}C NMR spectrum of $[H_2NEt_2]_2$[**7**] (chloroform-*d*, 100.6 MHz).

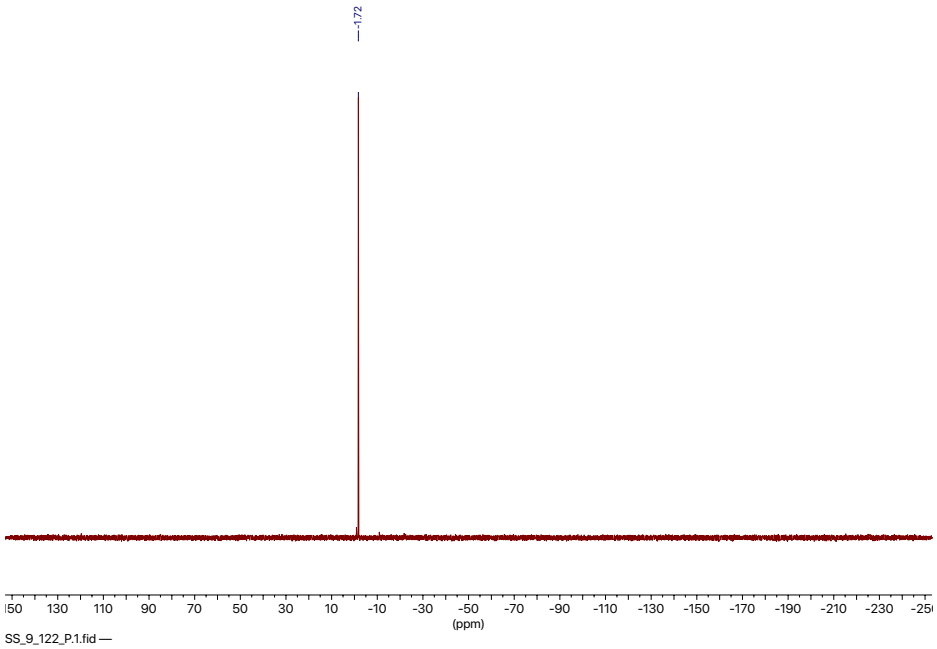

Figure S30: $^{31}P\{^{1}H\}$ NMR spectrum of $[H_2NEt_2]_2$[**7**] (chloroform-*d*, 162.0 MHz).

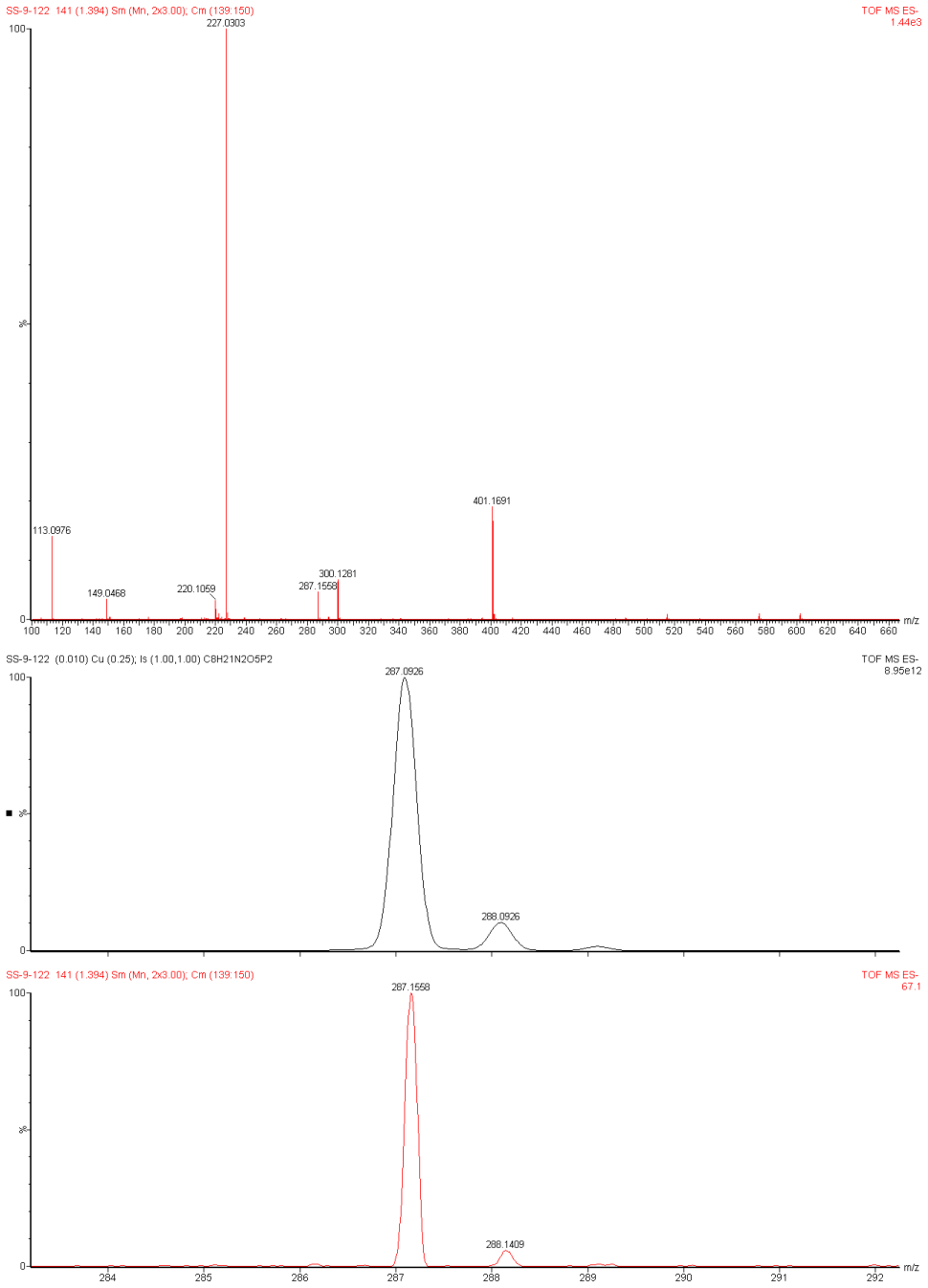

Figure S31: ESI-MS(−) of $[H_2NEt_2]_2$[**7**] (CH_3CN) with zoomed in portion showing the molecular ion ($[C_8H_{20}N_2O_5P_2]H^-$, bottom), and calculated isotope pattern (top).

2.9 Generation of 8 and 9 from 5

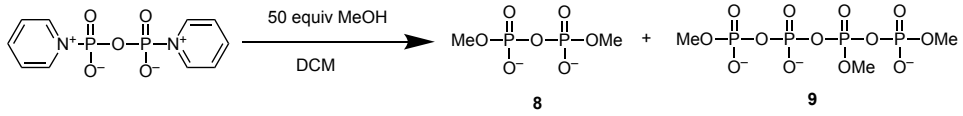

Figure S32: Treatment of **5** with MeOH to form **8** and **9**.

In the glovebox, **5** (0.11 g, 0.36 mmol) was suspended in dichloromethane (5 mL) in a Schlenk flask. The flask was then removed from the glovebox and attached to a Schlenk line. Against a flow of nitrogen, methanol (0.74 mL, 18.2 mmol) was added by syringe all at once. The mixture was stirred for 15 min and then filtered to remove insoluble material. Removing volatiles under reduced pressure left a colorless oil (0.066 g, 2:1 ratio of **8** to **9** by ^{1}H NMR integration).

2.9.1 Characterization data for 8

^{1}H NMR (D_2O, 400 MHz): δ 3.64 (d, J = 11.6 Hz, 6H).
^{13}C{^{1}H} NMR (D_2O, 100.6 MHz): δ 53.52 (t, J = 3.2 Hz).
^{31}P{^{1}H} NMR (D_2O, 162.0 MHz): δ −10.72.

2.9.2 Characterization data for 9

^{1}H NMR (D_2O, 400 MHz): δ 3.93 to 3.80 (m, 3H), 3.74 to 3.53 (m, 6H).
^{13}C{^{1}H} NMR (D_2O, 100.6 MHz): δ 53.96 (d, J = 7.0 Hz), 53.72 (d, J = 6.2 Hz), 53.08 (d, J = 5.5 Hz).
^{31}P{^{1}H} NMR (D_2O, 162.0 MHz): δ −11.65 (d, J = 17.0 Hz), −12.21 (d, J = 17.0 Hz), −23.68 (t, J = 16.4 Hz), −25.18 (t, J = 16.5 Hz).

2.9.3 Spectra for 8 and 9

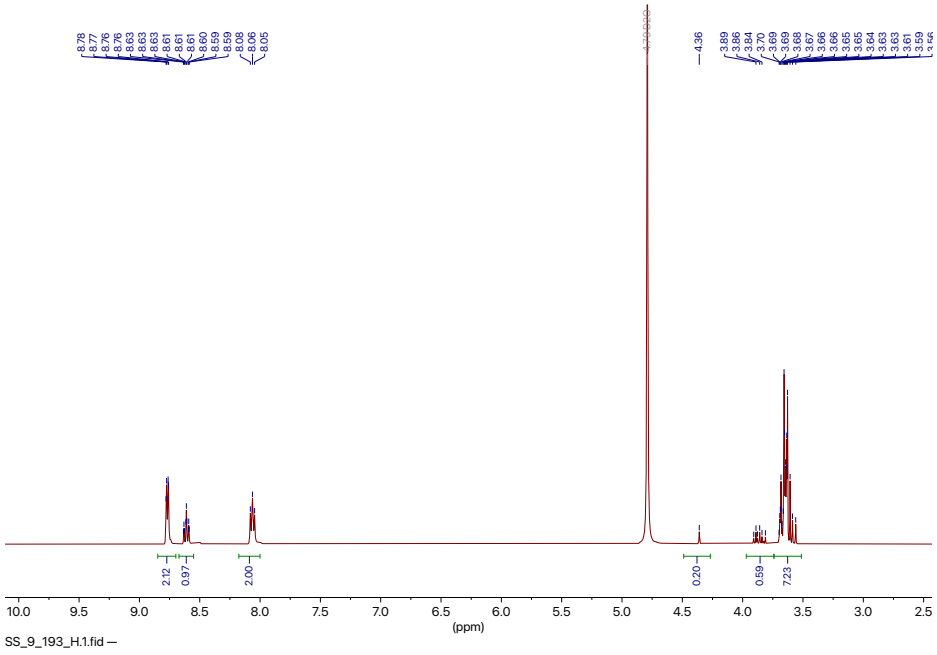

Figure S33: ^{1}H NMR spectrum of **8** and **9** (D_2O, 400 MHz).

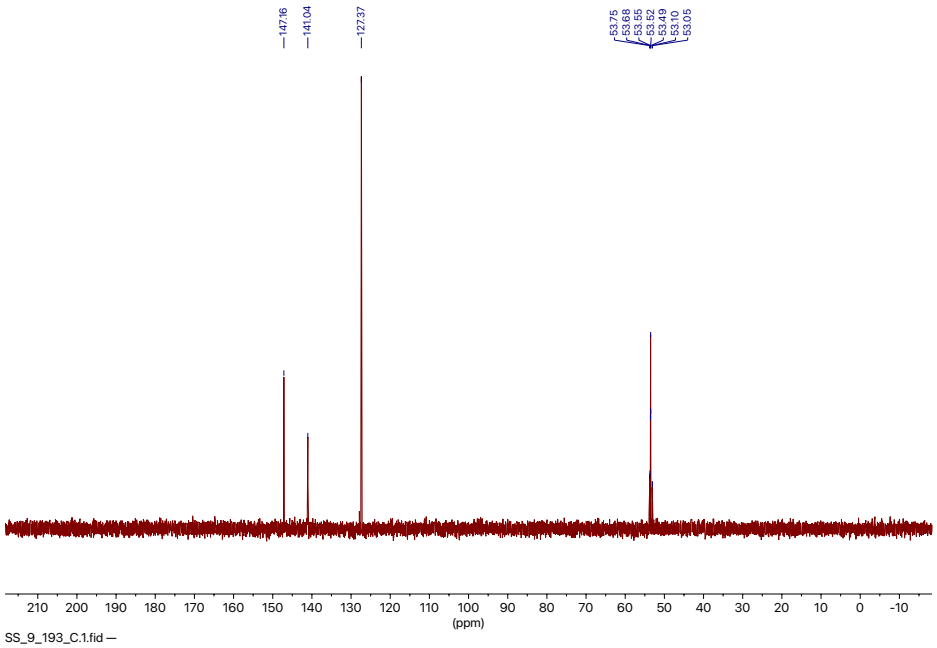

Figure S34: ^{13}C NMR spectrum of **8** and **9** (D_2O, 100.6 MHz).

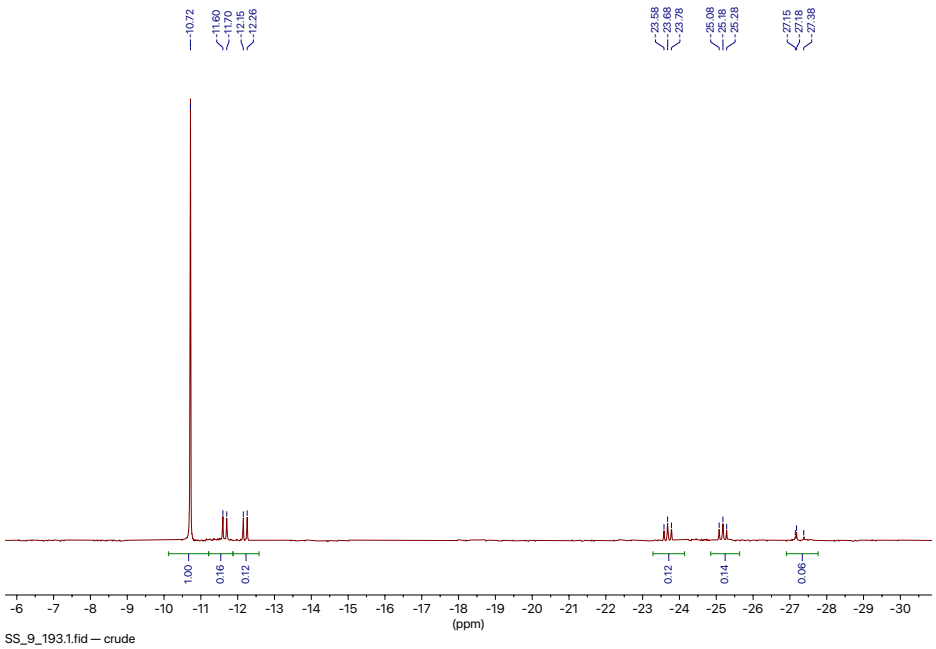

Figure S35: $^{31}P\{^{1}H\}$ NMR spectrum of **8** and **9** (D_2O, 162.0 MHz).

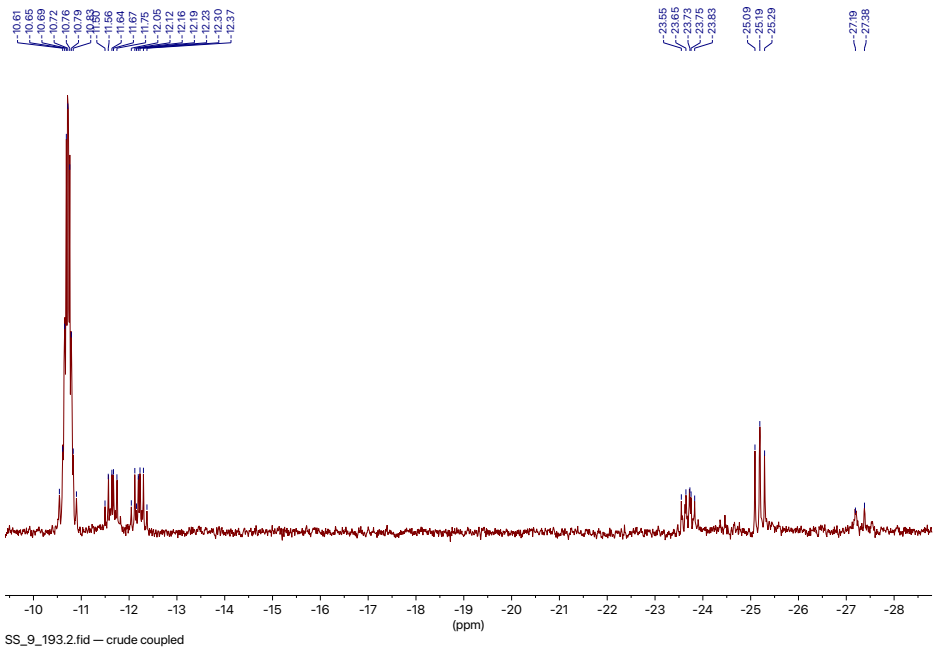

Figure S36: ^{31}P NMR spectrum of **8** and **9** (D_2O, 162.0 MHz).

2.10 Characterization of intermediate 10

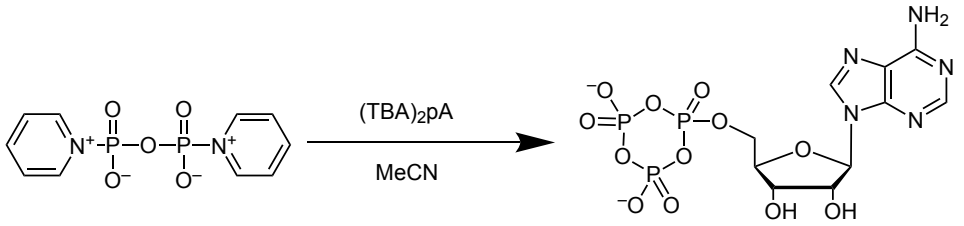

Figure S37: Formation of intermediate **10**.

In the glovebox, **5** (0.027, 0.089 mmol) was suspended in acetonitrile (1 mL). To this stirring suspension was added a 0.10 g/mL solution of $(TBA)_2pA$ in acetonitrile (0.74 mL, 0.089 mmol). After stirring for 5 min, all of the solid material had dissolved. $^{31}P\{^1H\}$ NMR of the resulting solution shows formation of **10** with only minor impurities.

$^{31}P\{^1H\}$ NMR (acetonitrile, 162.0 MHz): δ −22.32 (t, J = 25.1 Hz), −23.06 (dd, J = 28.7, 25.2 Hz), −24.08 (t, J = 26.8 Hz).

ESI-MS(−) of $[C_{10}H_{12}N_5O_{12}P_3]H^-$ (CH_3CN, m/z) 488.06 (calc'd 487.98)

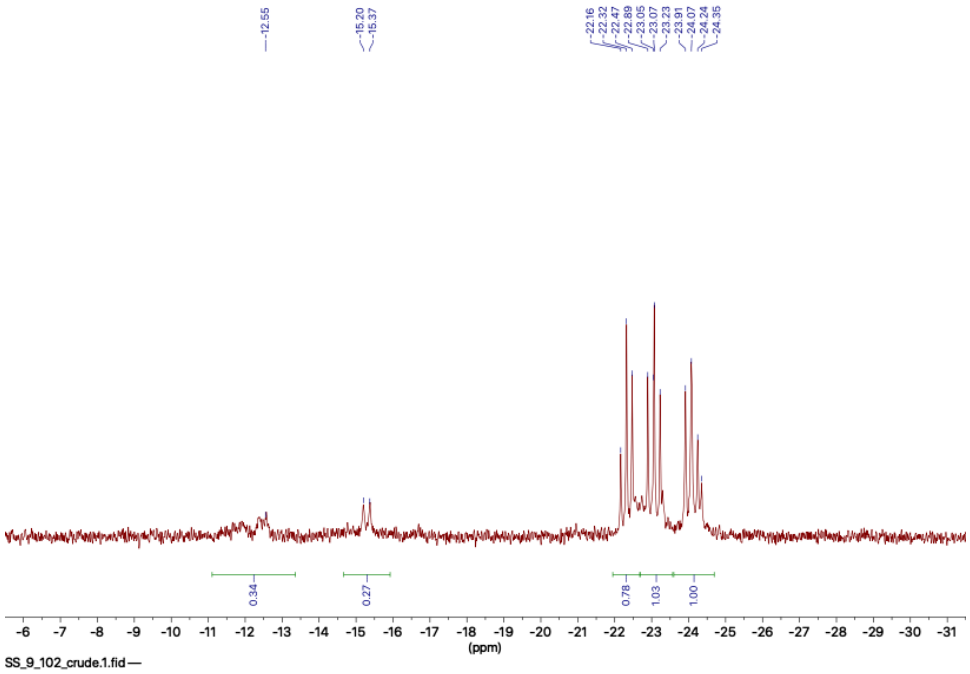

Figure S38: $^{31}P\{^1H\}$ NMR spectrum of **10** (acetonitrile, 162.0 MHz).

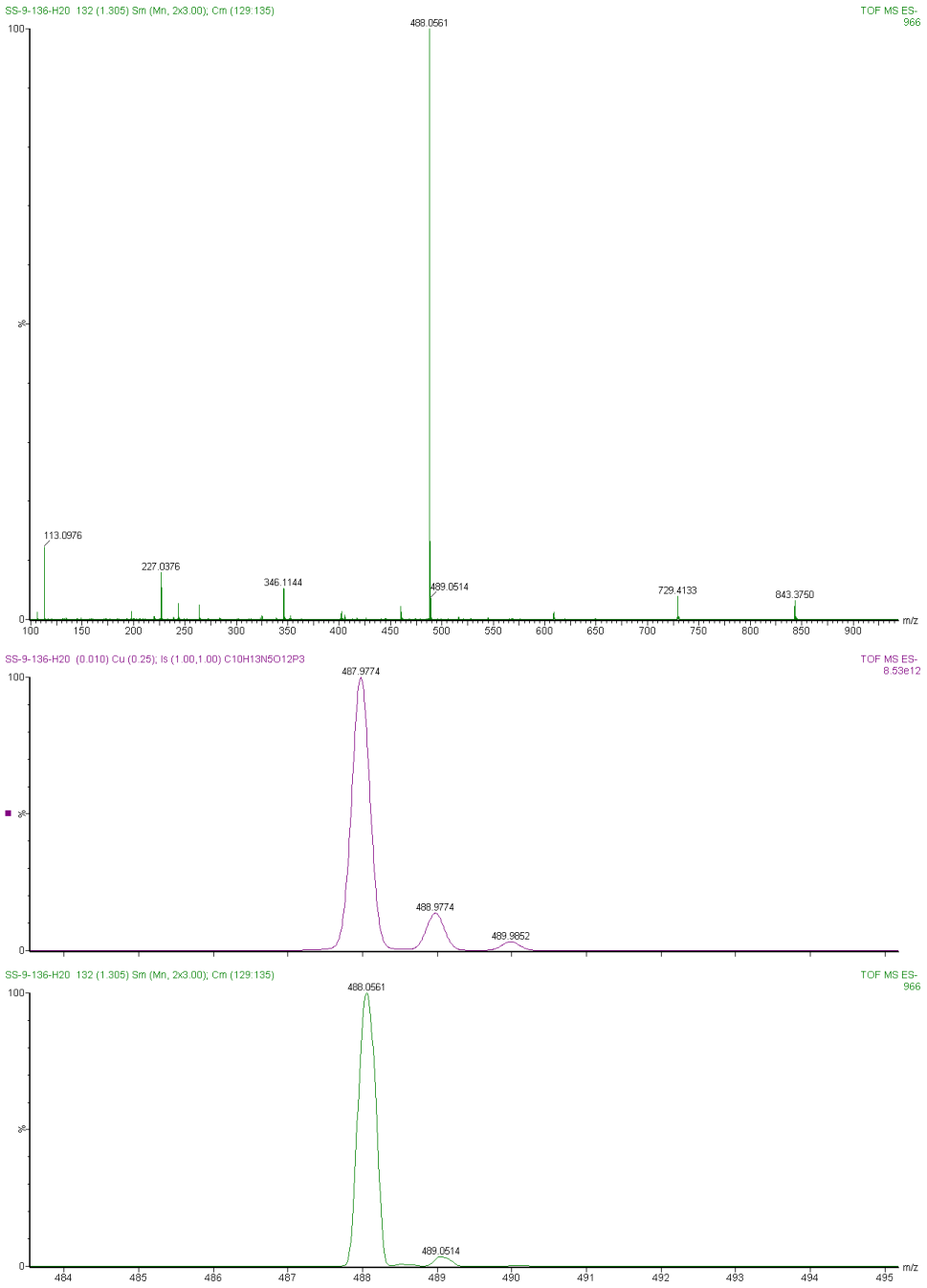

Figure S39: ESI-MS(−) of **10** (CH_3CN) with zoomed in portion showing the molecular ion ($[C_{10}H_{12}N_5O_{12}P_3]H^-$, bottom), and calculated isotope pattern (top).

2.11 Synthesis of $[NH_4]_4$[11]

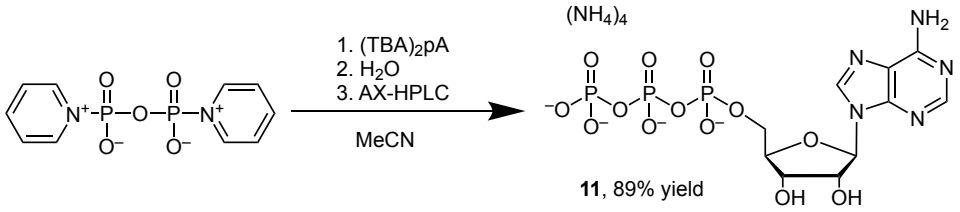

Figure S40: Synthesis of $[NH_4]_4$[**11**].

In a glovebox, **5** (0.0097 g, 0.032 mmol) was suspended in acetonitrile (1 mL). To this stirring suspension was added a 0.10 g/mL solution of $(TBA)_2$pA in acetonitrile (0.27 mL, 0.032 mmol). After stirring for 5 min, all of the solid material had dissolved. Volatiles were then evaporated under reduced pressure, leaving an oily solid. This residue was then removed from the glovebox and dissolved in deionized water (2 mL). The resulting solution was then filtered through an Acrodisc 0.2 μm wwPTFE syringe filter and purified by AX-HPLC according to the procedure in the General Considerations. The fractions containing the product were pooled and lyophilized. The resulting solid was again dissolved in deionized water and lyophilized giving the product as a fluffy white solid (0.016 g, 0.029 mmol, 89% yield).

The experimental characterization data for $[NH_4]_4$[**11**] is in good agreement with the literature data for ATP.[6]

^{1}H NMR (D_2O, 400 MHz): δ 8.50 (s, 1H), 8.26 (s, 1H), 6.14 (d, J = 5.7 Hz, 1H), 4.61 to 4.50 (m, 1H), 4.41 (t, J = 3.2 Hz, 1H), 4.27 (q, J = 5.2, 4.6 Hz, 2H).

^{13}C{^{1}H} NMR (D_2O, 100.6 MHz): δ 158.28, 155.54, 151.76, 142.54, 121.25, 89.47, 86.37, 76.77, 72.88, 67.88.

^{31}P{^{1}H} NMR (D_2O, 162.0 MHz): δ −5.91 (d, J = 14.6 Hz), −10.95 (d, J = 15.0 Hz), −19.35 (dd, J = 14.6, 15.0).

ESI-MS(−) of $[C_{10}H_{12}N_5O_{13}P_3]H_3^-$ ($(H_2O/MeCN)$, m/z) 505.99 (calc'd 505.99)

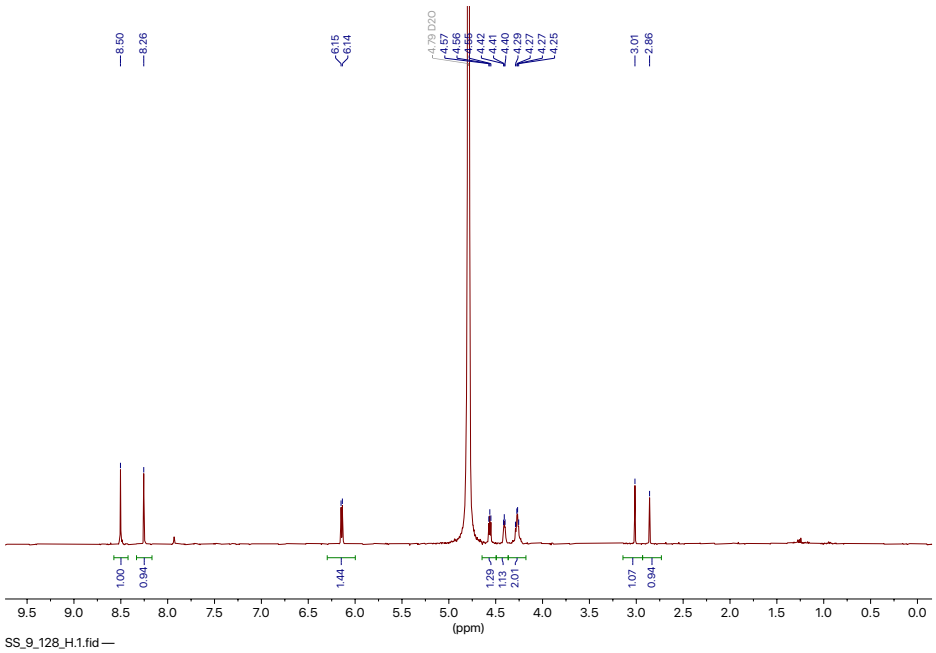

Figure S41: ^{1}H NMR spectrum of $[NH_4]_4$[**11**] (D_2O, 400 MHz).

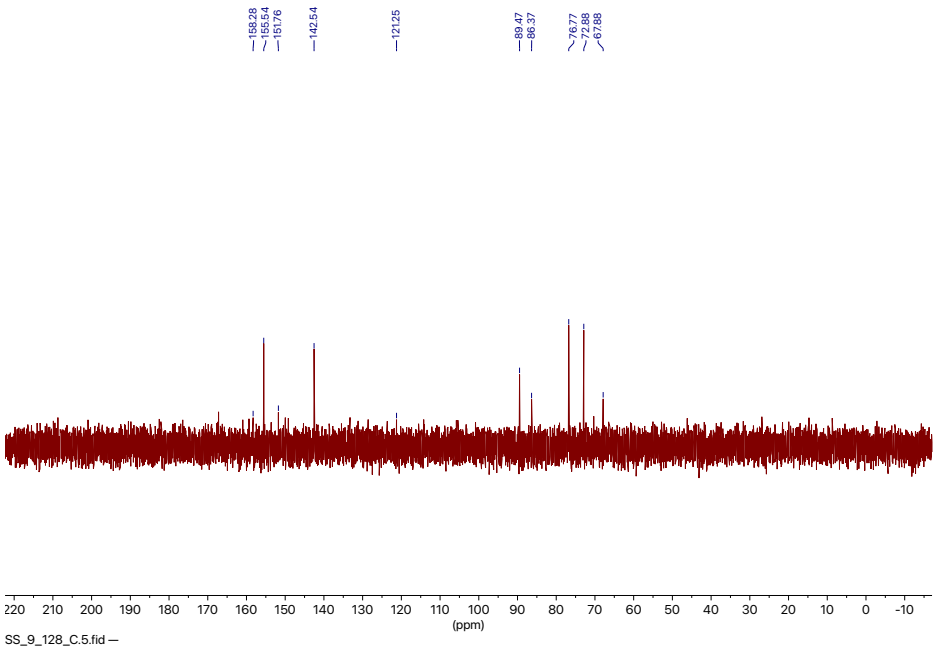

Figure S42: ^{13}C NMR spectrum of $[NH_4]_4$[**11**] (D_2O, 100.6 MHz).

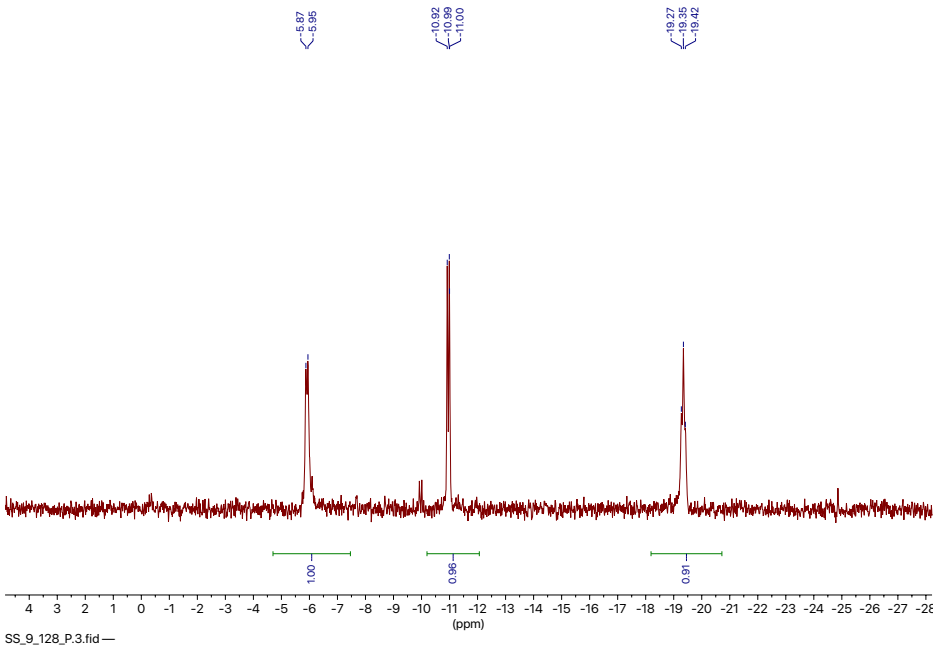

Figure S43: $^{31}P\{^{1}H\}$ NMR spectrum of $[NH_4]_4$[**11**] (D_2O, 162.0 MHz).

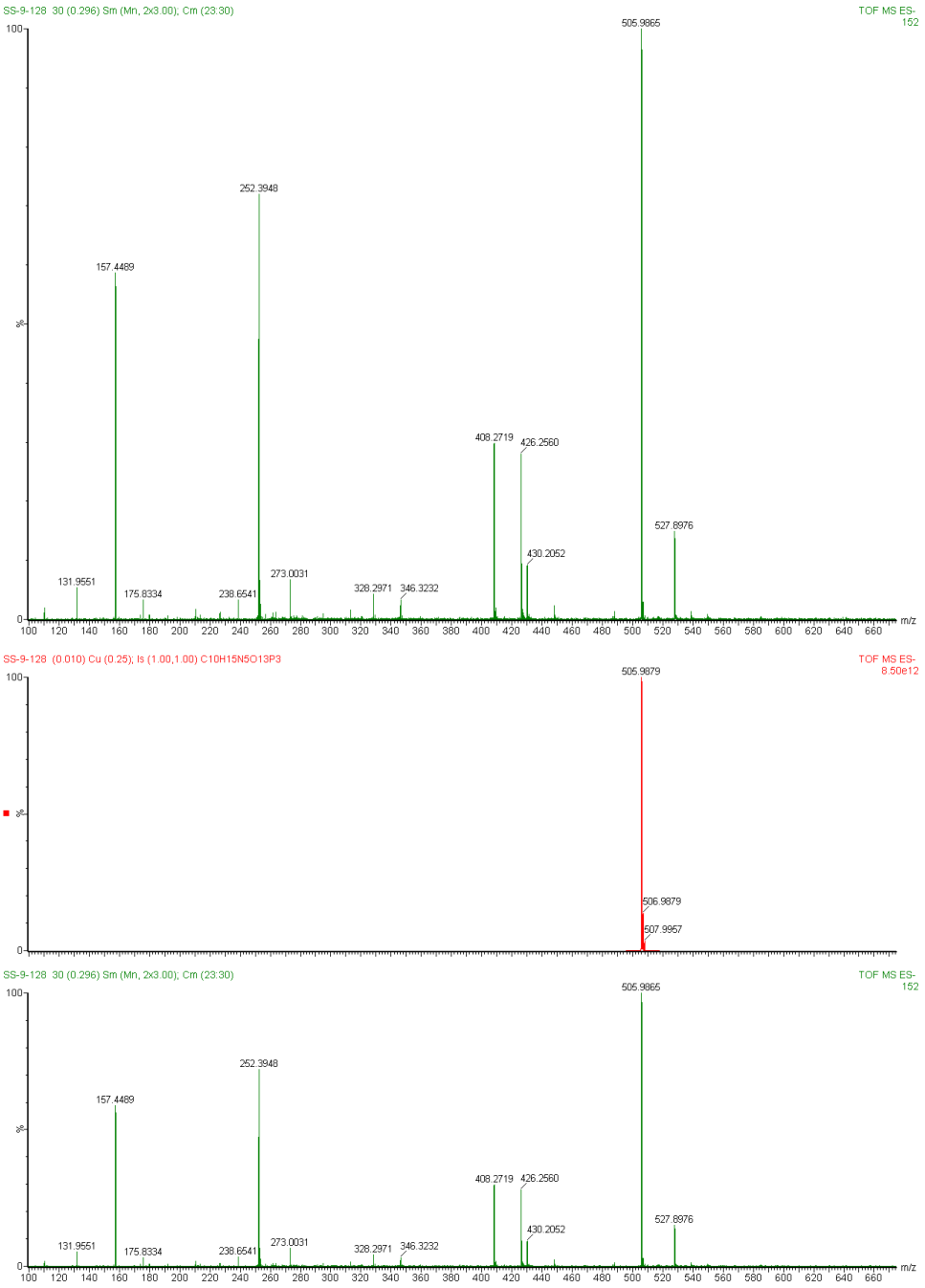

Figure S44: ESI-MS(−) of $[NH_4]_4$[**11**] (H_2O/MeCN) with zoomed in portion showing the molecular ion ($[C_{10}H_{14}N_5O_{13}P_3]H^-$, bottom), and calculated isotope pattern (top).

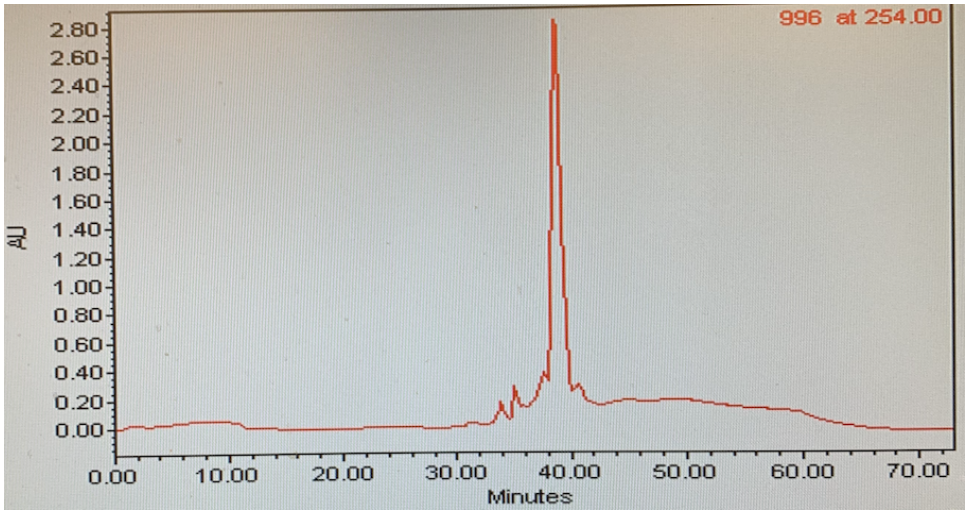

Figure S45: AX-HPLC trace of purified $[NH_4]_4$[**11**].

2.12 Synthesis of $[NH_4]_3$[12]

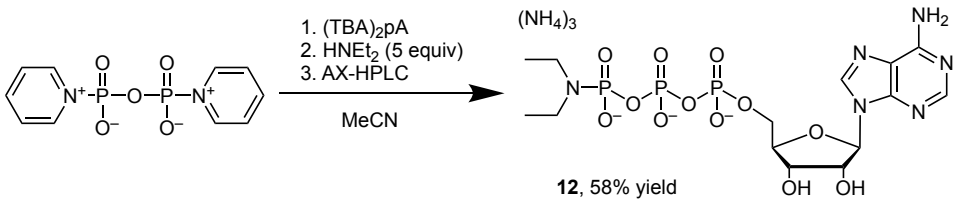

Figure S46: Synthesis of $[NH_4]_3$[**12**].

In a glovebox, **5** (0.012 g, 0.038 mmol) was suspended in acetonitrile (1 mL). To this stirring suspension was added a 0.10 g/mL solution of $(TBA)_2$pA in acetonitrile (0.31 mL, 0.038 mmol). After stirring for 5 min, all of the solid material had dissolved. To this solution was then added diethylamine (0.014 g, 0.19 mmol) in acetonitrile (1 mL). The resulting mixture was stirred for 6 hours, then volatiles were evaporated under reduced pressure, leaving an oily solid. This residue was then removed from the glovebox and dissolved in deionized water (2 mL). The resulting solution was then filtered through an Acrodisc 0.2 μm wwPTFE syringe filter and purified by AX-HPLC according to the procedure in the General Considerations. The fractions containing the product were pooled and lyophilized. The resulting solid was again dissolved in deionized water and lyophilized giving the product as a fluffy white solid (0.013 g, 0.022 mmol, 58% yield). After repeated lyophilizations of the product, the P–N bond was found to undergo hydrolysis, giving ATP as the primary phosphorus containing species.

^{1}H NMR (D_2O, 400 MHz): δ 8.47 (s, 1H), 8.24 (s, 1H), 6.12 (d, J = 5.6 Hz, 1H), 4.52 (t, J = 4.6 Hz, 1H), 4.38 (d, J = 3.4 Hz, 1H), 4.24 (t, J = 4.7 Hz, 2H), 2.96 (dq, J = 13.9, 7.1 Hz, 4H), 0.97 (t, J = 7.1 Hz, 6H).

^{31}P{^{1}H} NMR (D_2O, 162.0 MHz): δ 0.35 (d, J = 21.5 Hz), −11.06 (d, J = 14.6 Hz), −20.90 (dd, J = 21.5, 14.6 Hz).

ESI-MS(−) of $[C_{14}H_{22}N_6O_{12}P_3]H_2^-$ ($(H_2O/MeCN)$, m/z) 560.90 (calc'd 561.07)

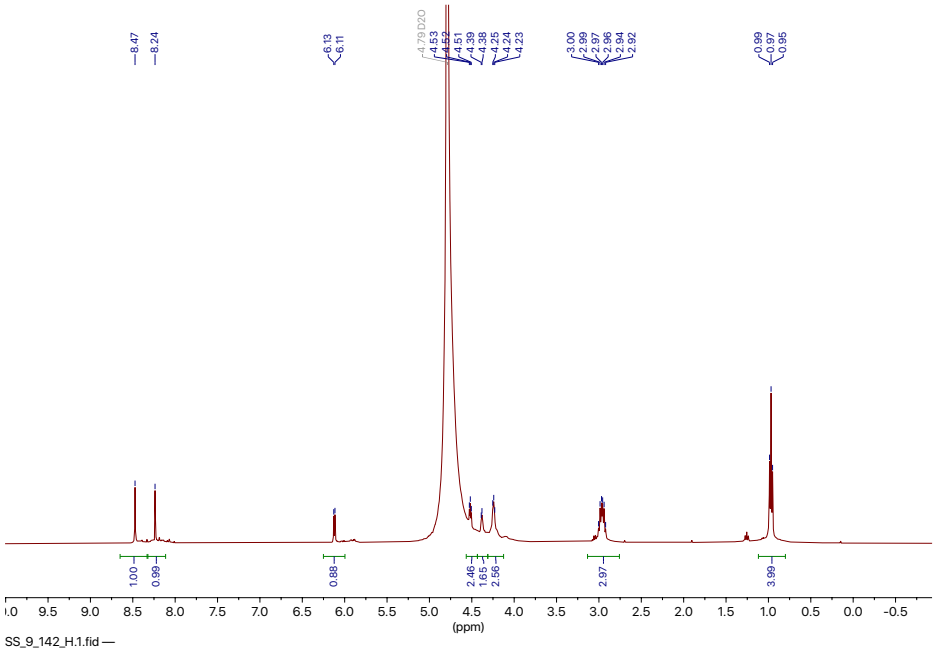

Figure S47: ^{1}H NMR spectrum of $[NH_4]_3$[**12**] (D_2O, 400 MHz).

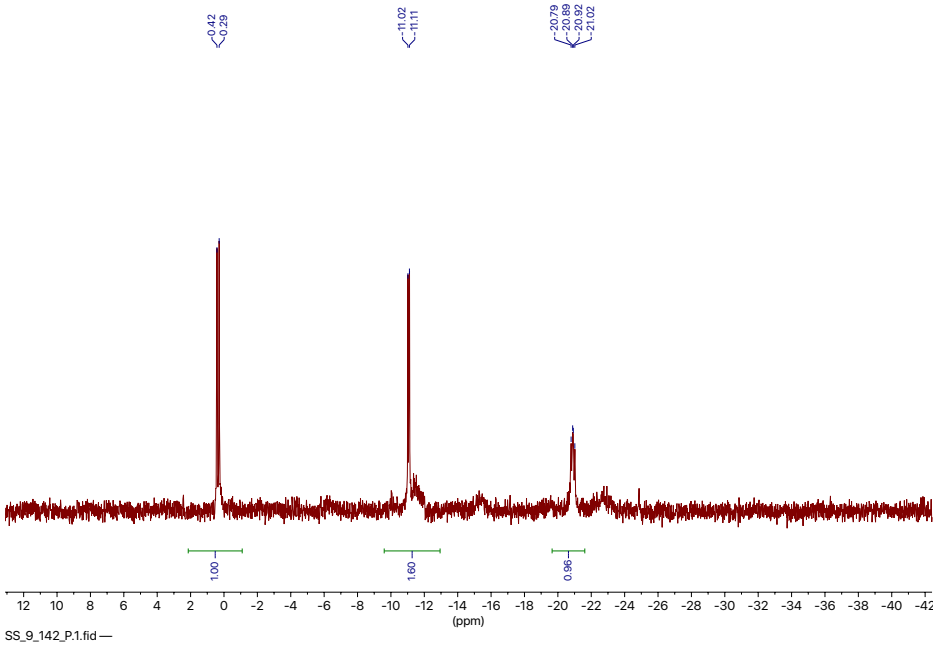

Figure S48: ^{31}P{^{1}H} NMR spectrum of $[NH_4]_3$[**12**] (D_2O, 162.0 MHz).

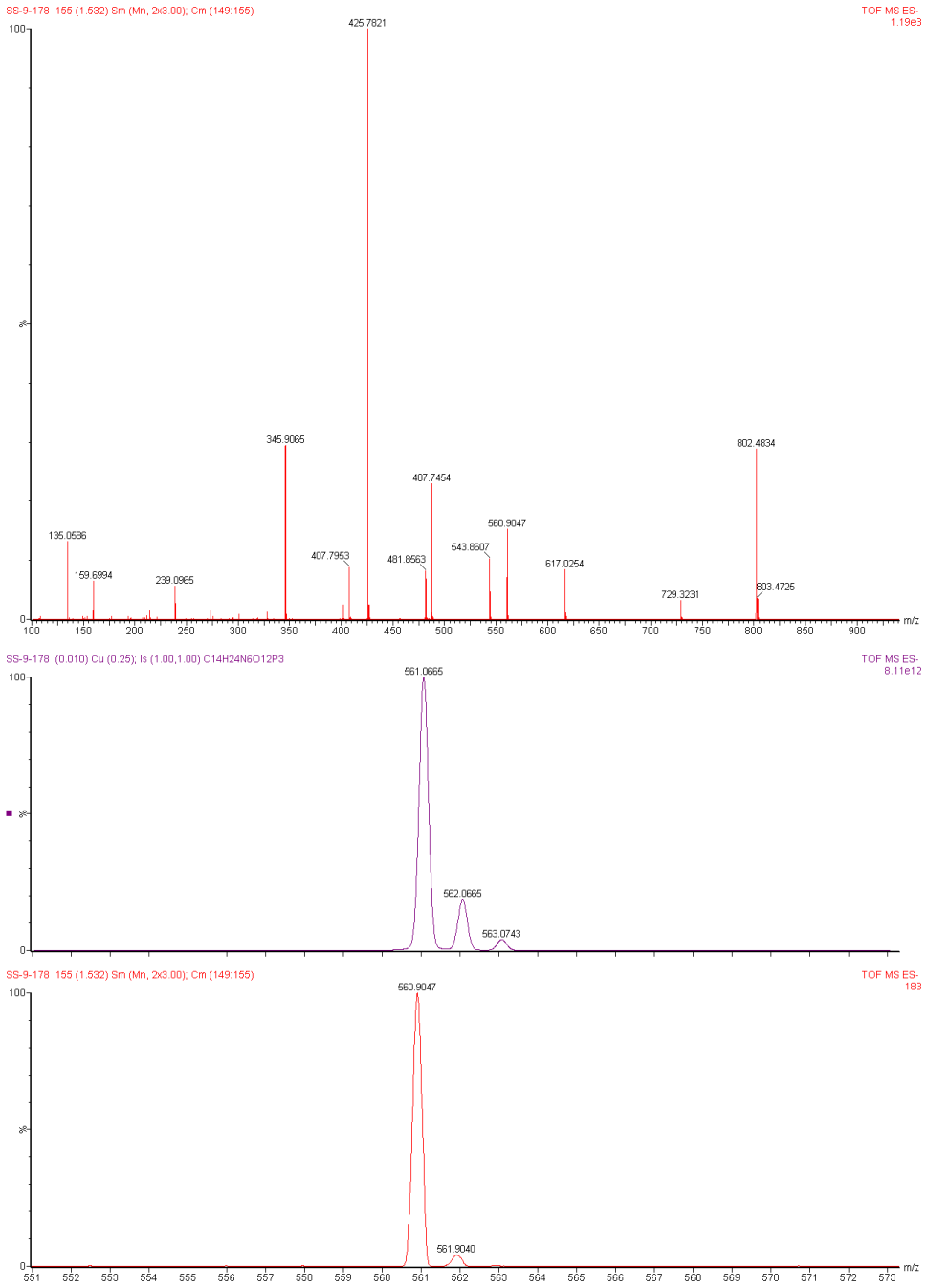

Figure S49: ESI-MS(−) of $[NH_4]_3$[**12**] (H_2O/MeCN) with zoomed in portion showing the molecular ion ($[C_{14}H_{23}N_6O_{12}P_3]H^-$, bottom), and calculated isotope pattern (top).

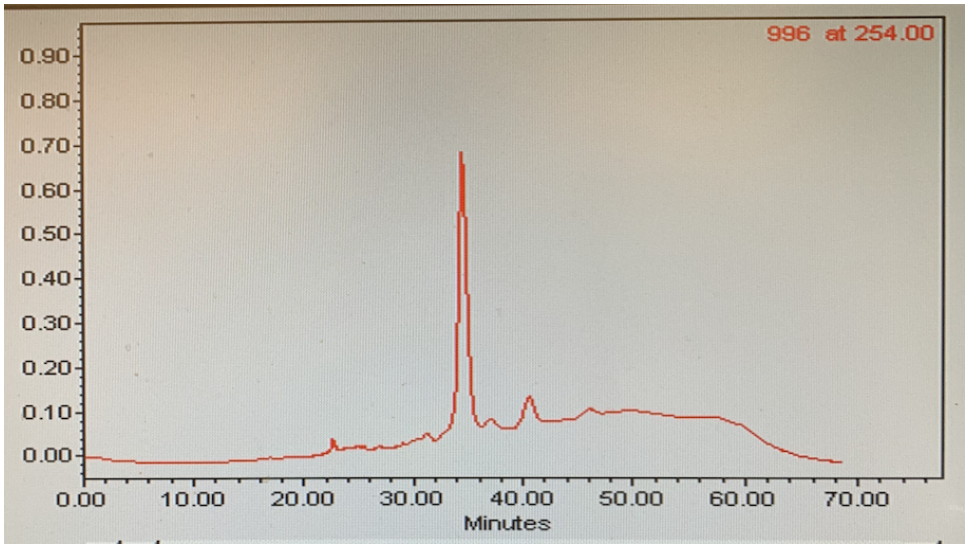

Figure S50: AX-HPLC trace of purified $[NH_4]_3$[**12**].

2.13 Synthesis of $[NH_4]_4$[13]

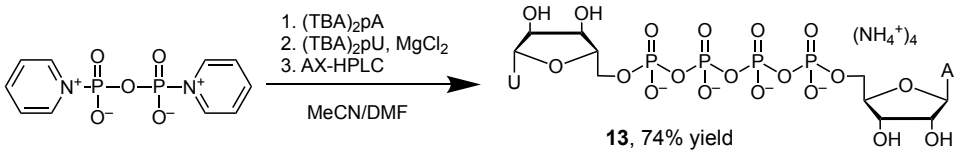

Figure S51: Synthesis of $[NH_4]_4$[**13**].

In a glovebox, **5** (0.011 g, 0.036 mmol) was suspended in acetonitrile (1 mL). To this stirring suspension was added a 0.10 g/mL solution of $(TBA)_2$pA in acetonitrile (0.30 mL, 0.036 mmol). After stirring for 5 min, all of the solid material had dissolved. Volatiles were then evaporated under reduced pressure, leaving an oily solid. This residue was then dissolved in DMF (1 mL). To this solution was added $MgCl_2$ (0.0068 g, 0.072 mmol) and a 0.10 g/mL solution of $(TBA)_2$pU in DMF (0.35 mL, 0.043 mmol). The resulting solution was stirred for 24 hours. Volatiles were then removed under reduced pressure at 40 °C leaving an oily solid. This residue was then removed from the glovebox and dissolved in deionized water (2 mL). The resulting solution was then filtered through an Acrodisc 0.2 μm wwPTFE syringe filter and purified by AX-HPLC according to the procedure in the General Considerations. The fractions containing the product were pooled and lyophilized. The resulting solid was again dissolved in deionized water and lyophilized giving the product as a fluffy white solid (0.023 g, 0.027 mmol, 74% yield).

The experimental characterization date for $[NH_4]_4$[**13**] is in good agreement with the literature data for Ap_4U.[7]

^{1}H NMR (D_2O, 400 MHz): δ 8.50 (s, 1H), 8.24 (s, 1H), 7.72 (d, J = 7.8 Hz, 1H), 6.13 (d, J = 5.7 Hz, 1H), 5.93 (d, J = 4.8 Hz, 1H), 5.83 (d, J = 7.8 Hz, 1H), 4.58 to 4.49 (m, 1H), 4.40 (d, J = 3.8 Hz, 1H), 4.36 to 4.15 (m, 8H).

$^{13}C\{^1H\}$ NMR (D_2O, 100.6 MHz): δ 169.06, 157.98, 155.83, 155.54, 151.73, 143.17, 142.52, 120.21, 105.52, 91.25, 89.53, 86.14, 85.20, 76.97, 76.32, 72.96, 72.24, 68.07, 67.84.

$^{31}P\{^1H\}$ NMR (D_2O, 162.0 MHz): δ −11.60 (m), −22.90 (m).

We had difficulty obtaining ESI-MS data for this compound due to low intensity of the MS signal. The best obtained MS data has very low signal to noise and does not show the expected molecular ion, which would be at m/z 826.03 for $[C_{20}H_{25}N_7O_{21}P_4]H_3^-$.

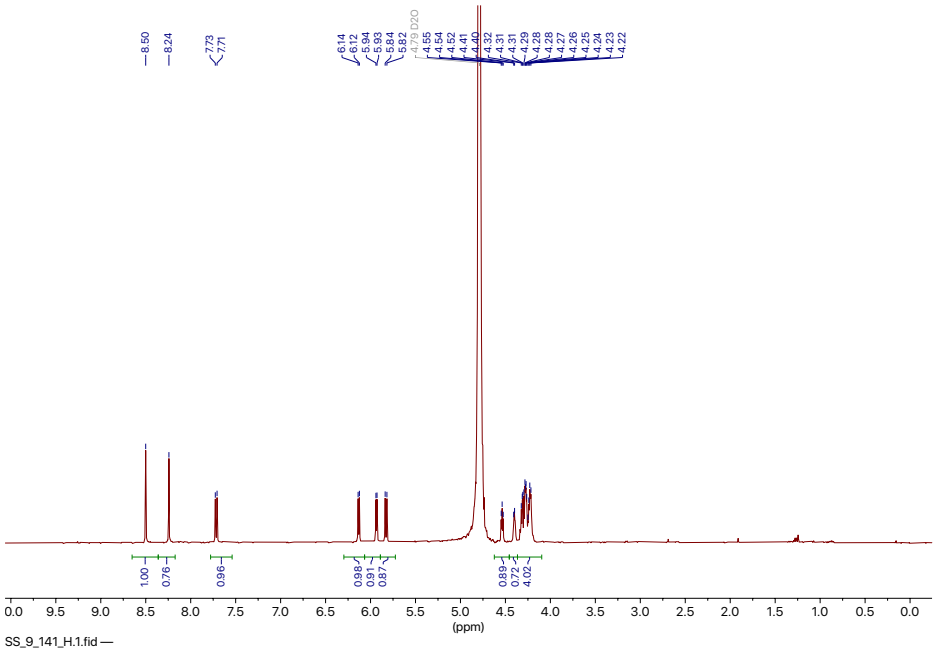

Figure S52: ^1H NMR spectrum of $[NH_4]_4$[**13**] (D_2O, 400 MHz).

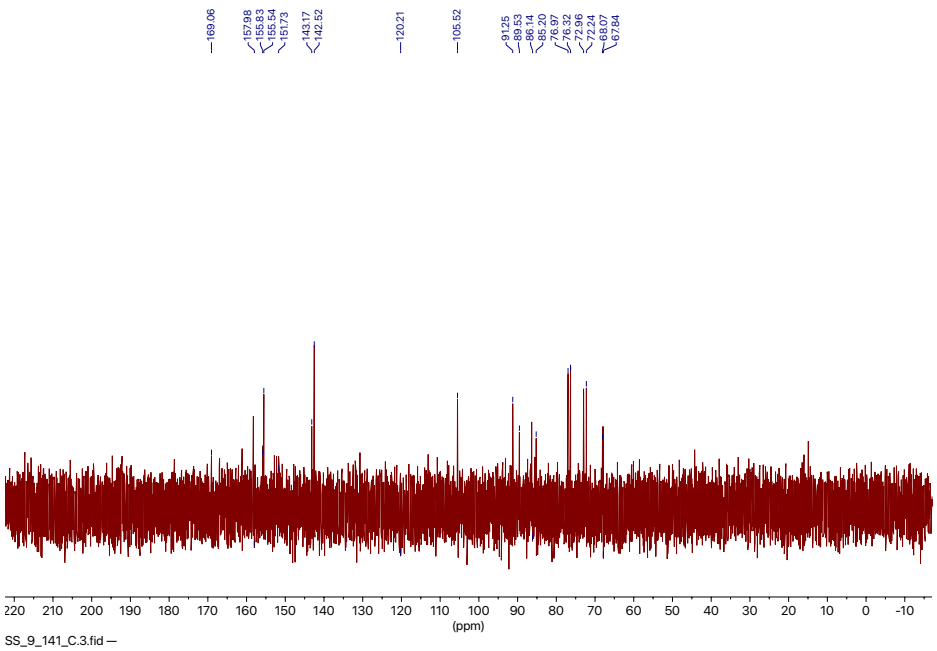

Figure S53: ^{13}C NMR spectrum of $[NH_4]_4$[**13**] (D_2O, 100.6 MHz).

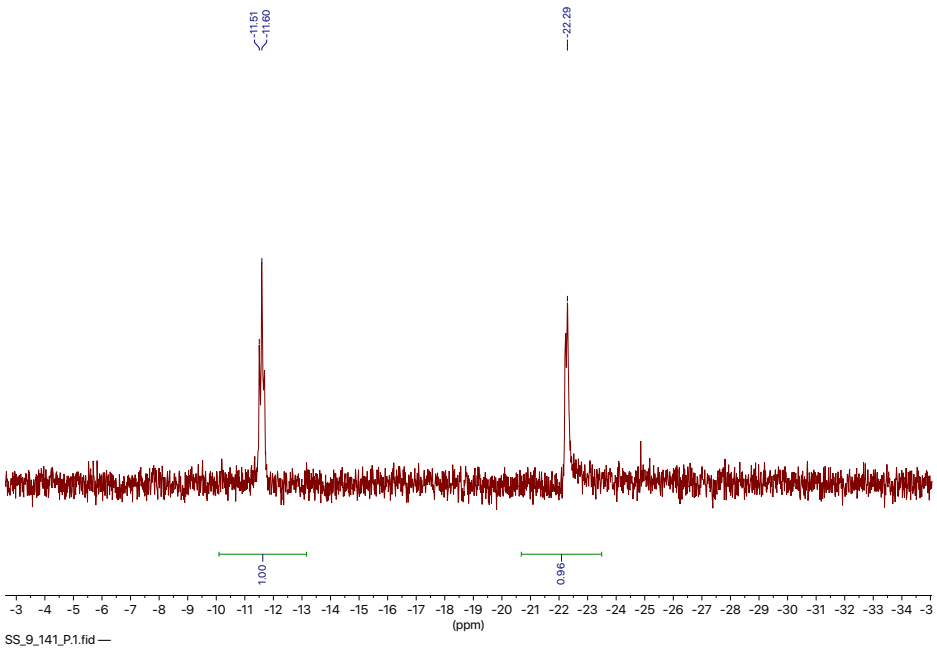

Figure S54: ^{31}P{^{1}H} NMR spectrum of $[NH_4]_4$[**13**] (D_2O, 162.0 MHz).

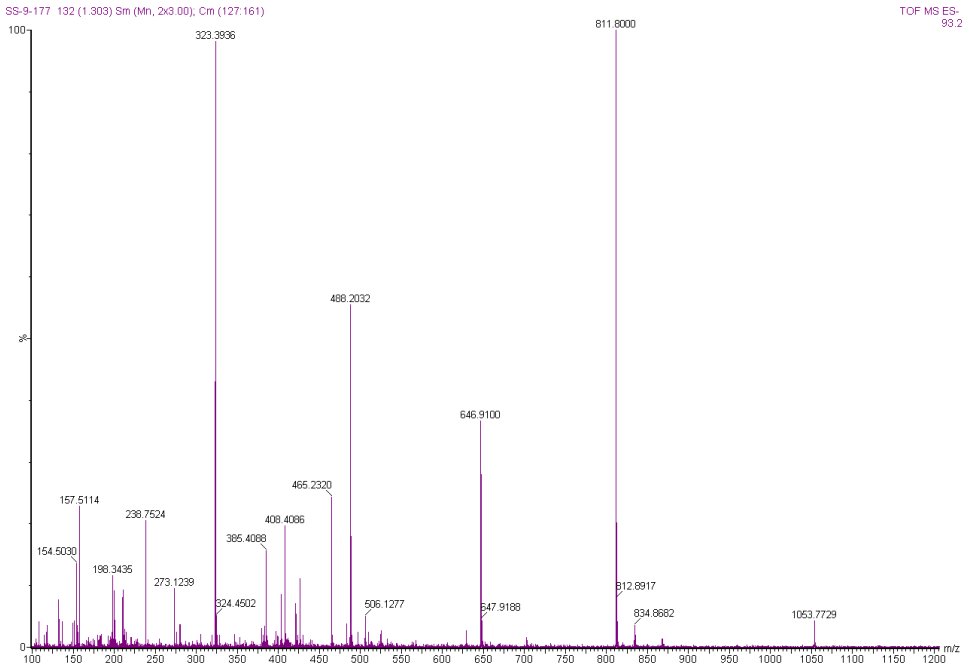

Figure S55: ESI-MS(−) of $[NH_4]_4$[**13**] (H_2O/MeCN).

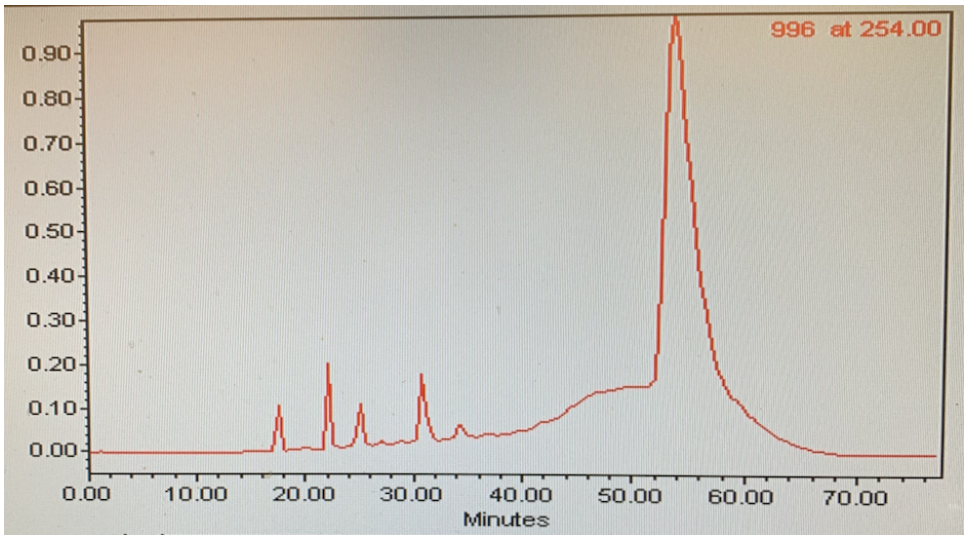

Figure S56: AX-HPLC trace of purified $[NH_4]_4$[**13**].

2.14 Synthesis of $[NH_4]_5$[14]

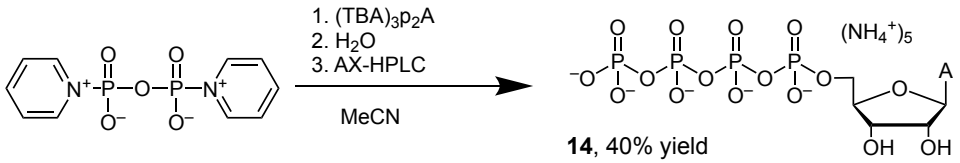

Figure S57: Synthesis of $[NH_4]_5$[**14**].

In a glovebox, **5** (0.013 g, 0.042 mmol) was suspended in acetonitrile (1 mL). To this stirring suspension was added a 0.10 g/mL solution of $(TBA)_3p_2A$ in acetonitrile (0.48 mL, 0.042 mmol). After stirring for 5 min, all of the solid material had dissolved. Volatiles were then evaporated under reduced pressure, leaving an oily solid. This residue was then removed from the glovebox and dissolved in deionized water (2 mL). The resulting solution was then filtered through an Acrodisc 0.2 μm wwPTFE syringe filter and purified by AX-HPLC according to the procedure in the General Considerations. The fractions containing the product were pooled and lyophilized. The resulting solid was again dissolved in deionized water and lyophilized giving the product as a fluffy white solid (0.011 g, 0.017 mmol, 40% yield).

^{1}H NMR (D_2O, 400 MHz): δ 8.50 (s, 1H), 8.25 (s, 1H), 6.14 (d, J = 5.9 Hz, 1H), 4.56 (dd, J = 5.1, 3.5 Hz, 1H), 4.49 to 4.36 (m, 1H), 4.27 (dt, J = 5.8, 3.3 Hz, 2H).

^{13}C{^{1}H} NMR (D_2O, 100.6 MHz): δ 155.63, 152.90, 149.14, 139.88, 118.58, 86.76, 83.82 (d, J = 9.2 Hz), 74.19, 70.37, 65.47.

^{31}P{^{1}H} NMR (D_2O, 162.0 MHz): δ −6.38 (d, J = 15.0 Hz), −11.71 (d, J = 16.6 Hz), −19.18 to −20.61 (m), −21.02 to −22.61 (m).

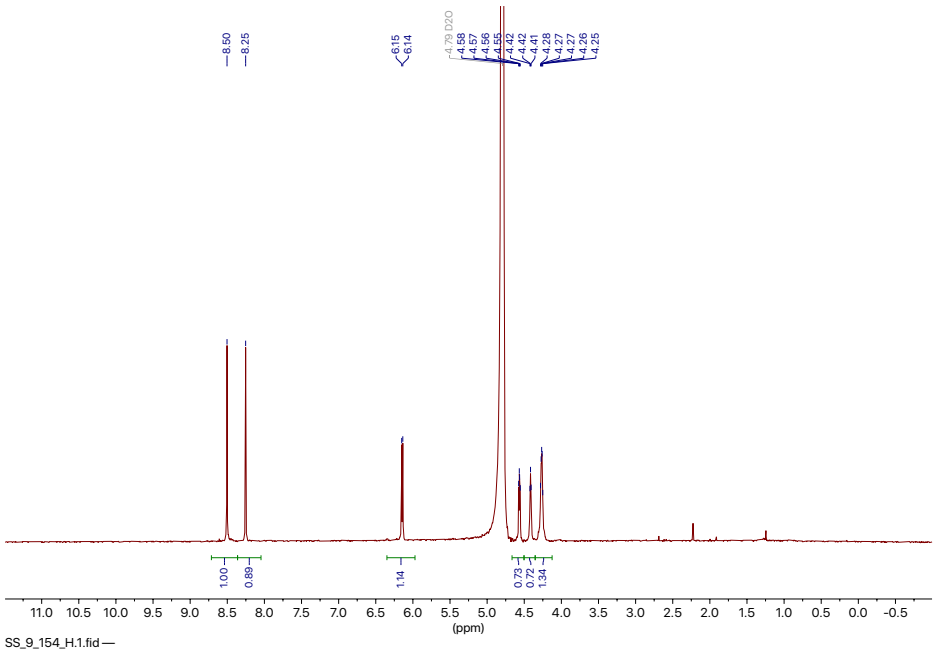

Figure S58: ^{1}H NMR spectrum of $[NH_4]_5$[**14**] (D_2O, 400 MHz).

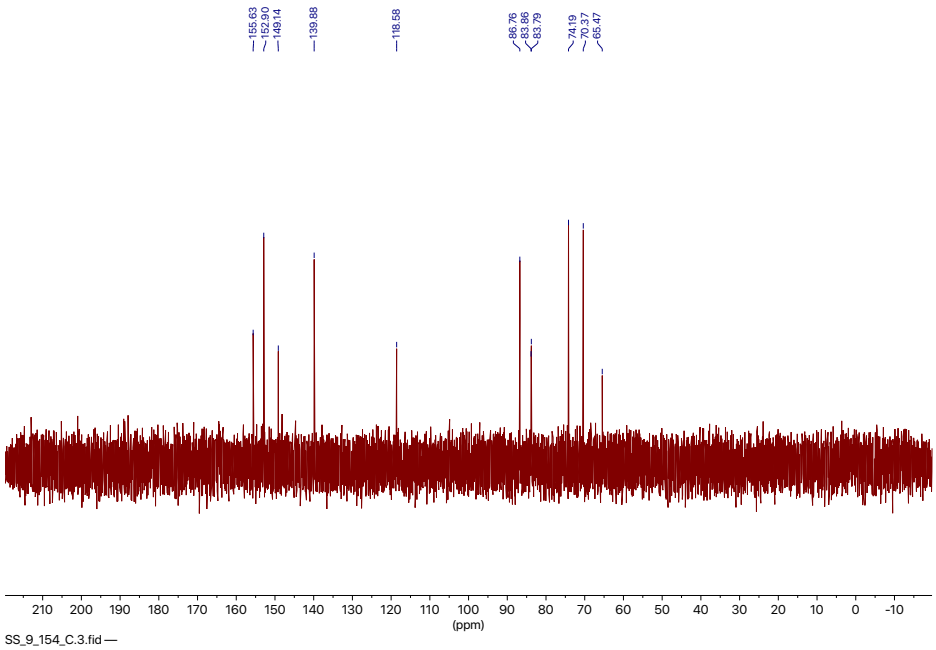

Figure S59: ^{13}C NMR spectrum of $[NH_4]_5$[**14**] (D_2O, 100.6 MHz).

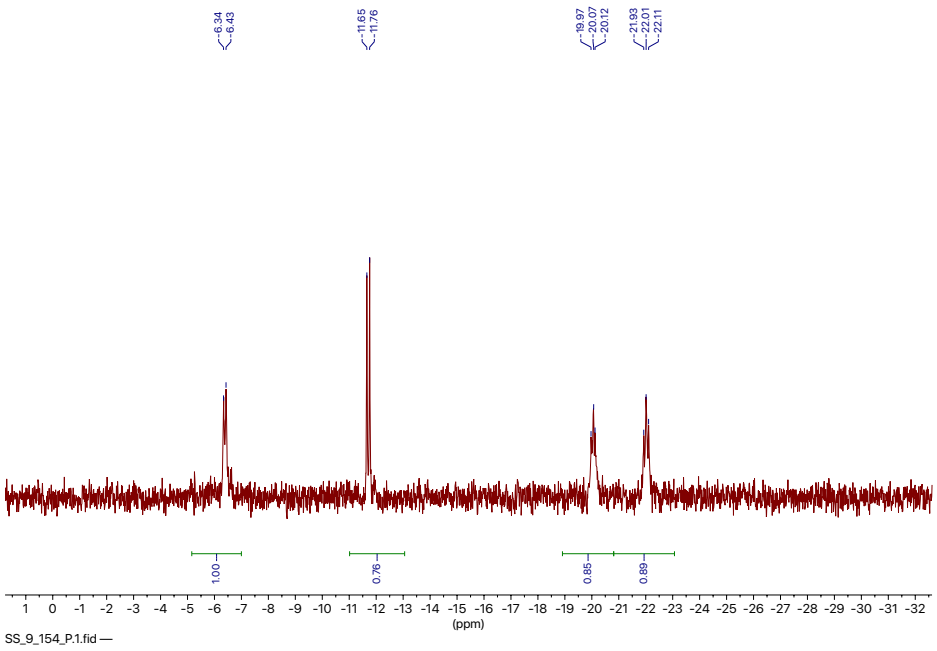

Figure S60: $^{31}P\{^{1}H\}$ NMR spectrum of $[NH_4]_5$[**14**] (D_2O, 162.0 MHz).

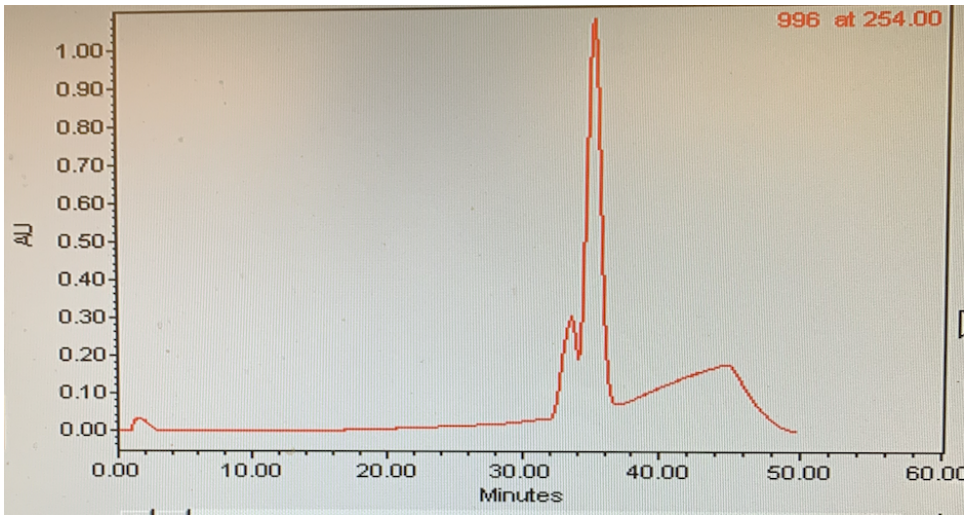

Figure S61: HPLC trace of purified $[NH_4]_5$[**14**].

3 Crystallographic Details

3.1 General Considerations

Crystals were mounted in hydrocarbon oil on a nylon fiber. Low-temperature (100 K) data were collected on a Bruker-AXS X8 Kappa Duo diffractometer coupled to a Smart Apex2 CCD detector with Cu κ_α radiation ($\lambda = 1.54178$ Å) or Mo κ_α radiation with ω- and ϕ- scans.

A semi-empirical absorption correction was applied to the diffraction data using SADABS.[8] All structures were solved by intrinsic phasing using SHELXT[9] and refined against F^2 on all data by full-matrix least squares with SHELXL-2015[10] using established methods. All non-hydrogen atoms were refined anisotropically. All hydrogen atoms were included in the model at geometrically calculated positions and refined using a riding model unless otherwise noted. The isotropic displacement parameters of all hydrogen atoms were fixed to 1.2 times the U_{eq} value of the atoms they are linked to (1.5 times for methyl groups). Descriptions of the individual refinements follow below and details of the data quality and a summary of the residual values of the refinements for all structures are given. Further details can be found in the form of .cif files available from the CCDC.

3.2 X-Ray Diffraction Study of [PPN][HNEt$_3$][1]

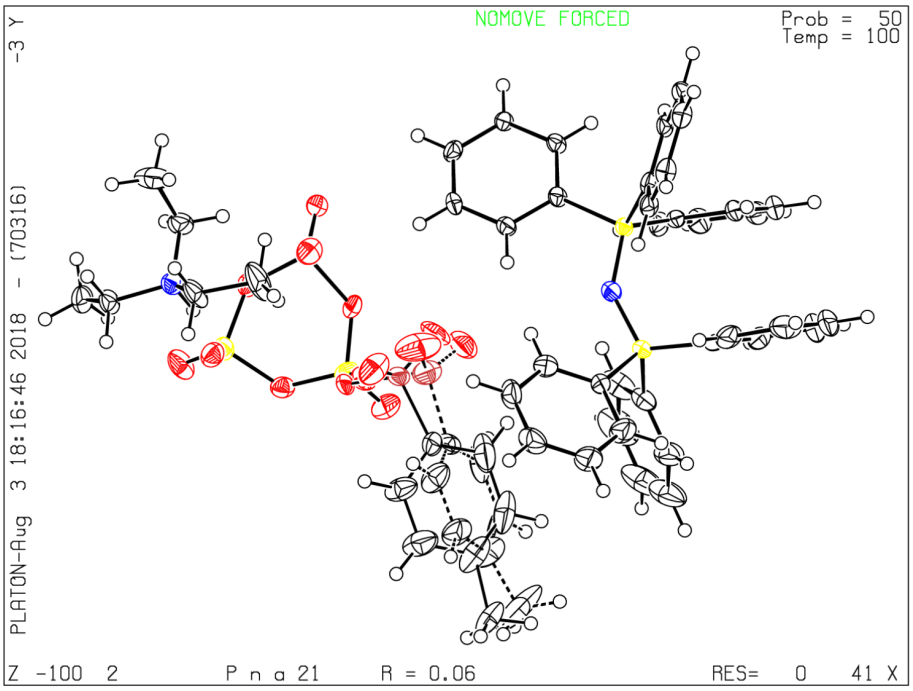

Figure S62: Single crystal X-ray Structure of [PPN][HNEt$_3$][**1**] with thermal ellipsoids set at 50%.

Colorless diffraction quality crystals of [PPN][HNEt$_3$][**1**] were grown by spontaneous precipitation from the acetone reaction mixture, as described in the synthetic section. The crystal was found to be significantly twinned. For the refinement, only the primary unit cell was used. There is one anomalous Q peak of about 1.4 electrons, near a phenyl ring of PPN. This was ignored. Additionally, checkcif notes an unusually low C–C bond precision. Therefore, this structure is best used to illustrate connectivity rather than to provide high precision bond metrics. The tosyl group was found to be disordered over two positions. The unusual Q peak could theoretically be a partially occupied water molecule.

Table S1: Crystallographic Table for [PPN][$HNEt_3$][**1**].

Identification code	[PPN][$HNEt_3$][1]	
CCDC Code	CCDC 2004821	
Empirical formula	$C_{49}H_{53}N_2O_{11}P_5S$	
Formula weight	1032.84	
Temperature	100(2) K	
Wavelength	1.54178 Å	
Crystal system	Orthorhombic	
Space group	$Pna2_1$	
Unit cell dimensions	a = 35.957(2) Å	$\alpha = 90°$.
	b = 14.6135(10) Å	$\beta = 90°$.
	c = 9.2973(6) Å	$\gamma = 90°$.
Volume	4885.3(6) Å^3	
Z	4	
Density (calculated)	1.404 Mg/m^3	
Absorption coefficient	2.661 mm^{-1}	
$F(000)$	2160	
Crystal size	0.460 × 0.200 × 0.040 mm^3	
Theta range for data collection	2.458 to 70.097°.	
Index ranges	-43<=h<=42, -17<=k<=17, -11<=l<=10	
Reflections collected	51484	
Independent reflections	8704 [R_{int} = 0.0540]	
Completeness to theta = 67.679°	99.4 %	
Absorption correction	Semi-empirical from equivalents	
Refinement method	Full-matrix least-squares on F^2	
Data / restraints / parameters	8704 / 964 / 718	
Goodness-of-fit on F^2	1.106	
Final R indices [I>2σ(I)]	R_1 = 0.0552, wR_2 = 0.1390	
R indices (all data)	R_1 = 0.0572, wR_2 = 0.1402	
Extinction coefficient	n/a	
Largest diff. peak and hole	1.377 and -0.396 eÅ^{-3}	

3.3 X-Ray Diffraction Study of 3

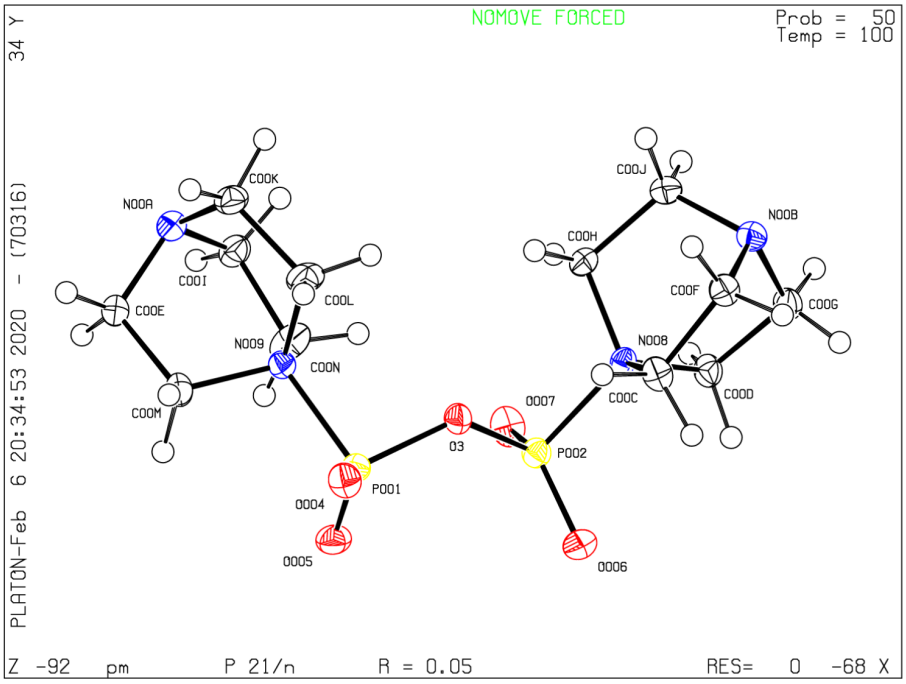

Figure S63: Single crystal X-ray Structure of **3** with thermal ellipsoids set at 50%.

Colorless crystals of a mixture of **3** and **4** were prepared by spontaneous precipitation from the reaction medium as described above. Carefully selecting crystals from the mixture allowed for an X-ray diffraction study of each component of the mixture.

Table S2: Crystallographic Table for **3**.

CCDC Code	CCDC 2071686	
Empirical formula	$C_{12}H_{24}N_4O_5P_2$	
Formula weight	366.29	
Temperature	100(2) K	
Wavelength	0.71073 Å	
Crystal system	Monoclinic	
Space group	P21/n	
Unit cell dimensions	a = 6.6073(5) Å	$\alpha = 90°$.
	b = 22.4113(14) Å	$\beta = 104.587(2)°$
	c = 10.5719(7) Å	$\gamma = 90°$
Volume	1515.01(18) Å^3	
Z	4	
Density (calculated)	1.606 Mg/m^3	
Absorption coefficient	0.320 mm^{-1}	
$F(000)$	776	
Crystal size	0.100 x 0.090 x 0.040 mm^3	
Theta range for data collection	1.817 to 30.562°	
Index ranges	-9<=h<=9, -32<=k<=32, -15<=l<=15	
Reflections collected	270093	
Independent reflections	4641 [R_{int} = 0.1474]	
Completeness to theta = 25.242°	99.9 %	
Absorption correction	None	
Refinement method	Full-matrix least-squares on F^2	
Data / restraints / parameters	4641 / 225 / 208	
Goodness-of-fit on F^2	1.095	
Final R indices [I>2σ(I)]	R_1 = 0.0469, wR_2 = 0.1113	
R indices (all data)	R_1 = 0.0756, wR_2 = 0.1294	
Extinction coefficient	n/a	
Largest diff. peak and hole	0.695 and -0.435 eÅ^{-3}	

3.4 X-Ray Diffraction Study of 4

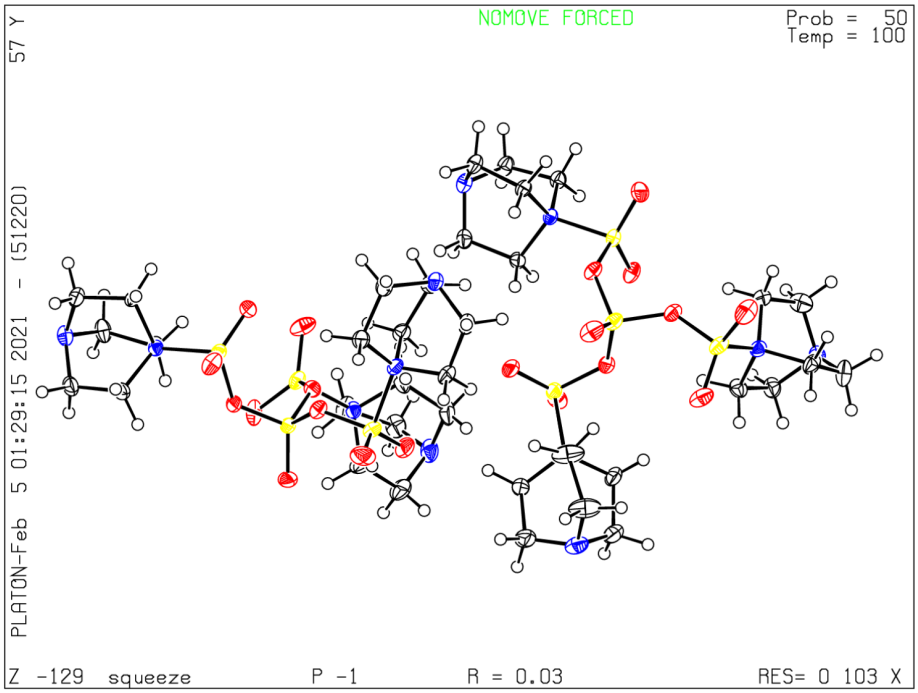

Figure S64: Single crystal X-ray Structure of **4** with thermal ellipsoids set at 50% probability and hydrogen atoms omitted for clarity.

Colorless crystals of a mixture of **3** and **4** were prepared by spontaneous precipitation from the reaction medium as described above. The structure of **4** contains a large amount of highly disordered acetonitrile molecules in the asymmetric unit. This density could not be satisfactorily modeled with discrete acetonitrile molecules and instead SQUEEZE was implemented in PLATON.[11]

Table S3: Crystallographic Table for **4**.

CCDC Code	CCDC 2059218	
Empirical formula	$C_{22.50}H_{46.50}N_7O_{10}P_4$	
Formula weight	699.04	
Temperature	100(2) K	
Wavelength	0.71073 Å	
Crystal system	Triclinic	
Space group	P−1	
Unit cell dimensions	a = 11.3678(3) Å	α = 78.0710(10)°.
	b = 16.7742(5) Å	β = 88.6850(10)°
	c = 16.9182(5) Å	γ = 88.3790(10)°
Volume	3154.65(16) Å^3	
Z	4	
Density (calculated)	1.472 Mg/m^3	
Absorption coefficient	0.303 mm^{-1}	
$F(000)$	1482	
Crystal size	0.510 x 0.200 x 0.175 mm^3	
Theta range for data collection	1.557 to 29.575°.	
Index ranges	-15<=h<=14, -23<=k<=23, -23<=l<=23	
Reflections collected	154058	
Independent reflections	17694 [R$_{int}$ = 0.0361]	
Completeness to theta = 25.242°	99.9 %	
Absorption correction	Semi-empirical from equivalents	
Refinement method	Full-matrix least-squares on F2	
Data / restraints / parameters	17694 / 896 / 685	
Goodness-of-fit on F^2	1.021	
Final R indices [I>2σ(I)]	R_1 = 0.0335, wR_2 = 0.0894	
R indices (all data)	R_1 = 0.0396, wR_2 = 0.0935	
Extinction coefficient	n/a	
Largest diff. peak and hole	0.543 and -0.519 eÅ^{-3}	

3.5 X-Ray Diffraction Study of $[H_2NEt_2]_2$[6]

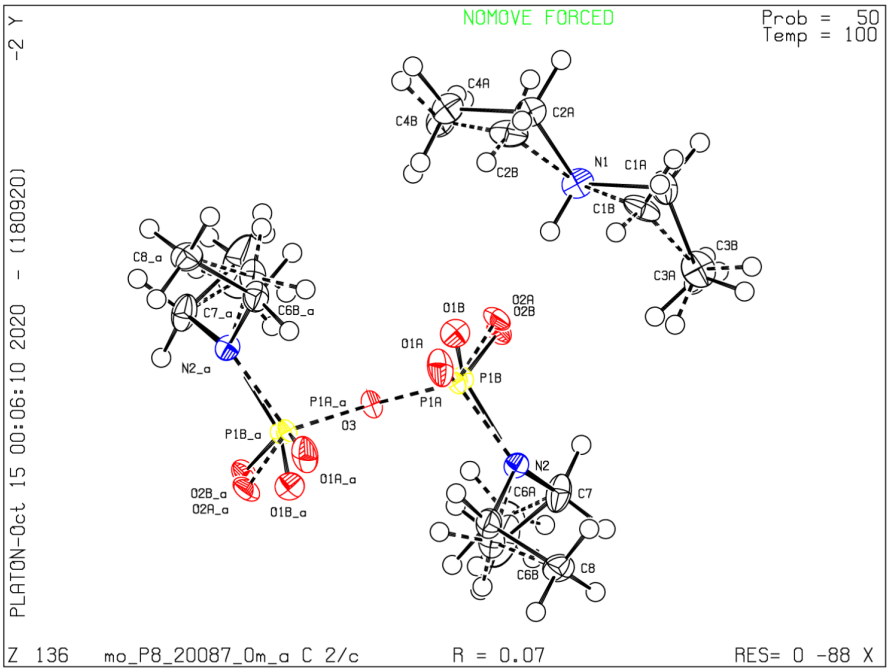

Figure S65: Single crystal X-ray Structure of **6** with thermal ellipsoids set at 50% probability and hydrogen atoms omitted for clarity.

Colorless crystals of $[H_2NEt_2]_2$[**6**] were grown by addition of diethyl ether to a dichloromethane solution of $[H_2NEt_2]_2$[**6**] in the glovebox. The data quality is not great due to poor crystal quality. There is also significant disorder in the crystal. Every atom was modeled over two positions except the nitrogen and one of the terminal oxygens, all of which seem well behaved. In the structure, each diethylammonium counterion is hydrogen bonded to the terminal oxygen of one phosphate as well as the other terminal oxygen of another molecule resulting in a infinite hydrogen bonding network.

Table S4: Crystallographic Table for $[H_2NEt_2]_2$**[6]**.

CCDC Code	CCDC 2071687	
Empirical formula	$C_{16}H_{44}N_4O_5P_2$	
Formula weight	434.49	
Temperature	100(2) K	
Wavelength	0.71073 Å	
Crystal system	Monoclinic	
Space group	C2/c	
Unit cell dimensions	a = 15.5842(7) Å	$\alpha = 90°$
	b = 8.5789(3) Å	$\beta = 108.014(2)°$
	c = 19.0349(8) Å	$\gamma = 90°$
Volume	2420.13(17) Å^3	
Z	4	
Density (calculated)	1.192 Mg/m^3	
Absorption coefficient	0.210 mm^{-1}	
$F(000)$	952	
Crystal size	0.265 x 0.130 x 0.095 mm^3	
Theta range for data collection	2.250 to 30.582°	
Index ranges	-22<=h<=22, -12<=k<=12, -27<=l<=27	
Reflections collected	51786	
Independent reflections	3729 [R_{int} = 0.0629]	
Completeness to theta = 25.242°	100.0 %	
Absorption correction	Semi-empirical from equivalents	
Refinement method	Full-matrix least-squares on F^2	
Data / restraints / parameters	3729 / 403 / 215	
Goodness-of-fit on F^2	1.271	
Final R indices [I>2σ(I)]	R_1 = 0.0719, wR_2 = 0.1577	
R indices (all data)	R_1 = 0.0752, wR_2 = 0.1591	
Extinction coefficient	n/a	
Largest diff. peak and hole	0.481 and -0.422 eÅ^{-3}	

References

[1] Pangborn, A. B.; Giardello, M. A.; Grubbs, R. H.; Rosen, R. K.; Timmers, F. J. Safe and convenient procedure for solvent purification. *Organometallics* **1996**, *15*, 1518–1520.

[2] Riddick, J. A. *Techniques of Chemistry. Organic Solvents. Physical Properties and Methods of Purification*; Wiley Interscience, 1970.

[3] Mohamady, S.; Taylor, S. D. Synthesis of nucleoside 5'-tetraphosphates containing terminal fluorescent labels via activated cyclic trimetaphosphate. *J. Org. Chem.* **2014**, *79*, 2308–2313.

[4] Chakarawet, K.; Knopf, I.; Nava, M.; Jiang, Y.; Stauber, J. M.; Cummins, C. C. Crystalline Metaphosphate Acid Salts: Synthesis in Organic Media, Structures, Hydrogen-Bonding Capability, and Implication of Superacidity. *Inorg. Chem.* **2016**, *55*, 6178–6185.

[5] Mohamady, S.; Taylor, S. D. Synthesis of nucleoside tetraphosphates and dinucleoside pentaphosphates via activation of cyclic trimetaphosphate. *Org. Lett.* **2013**, *15*, 2612–2615.

[6] Wishart, D. S.; Knox, C.; Guo, A. C.; Eisner, R.; Young, N.; Gautam, B.; Hau, D. D.; Psychogios, N.; Dong, E.; Bouatra, S., et al. HMDB: a knowledgebase for the human metabolome. *Nucleic Acids Res.* **2009**, *37*, D603–D610.

[7] Mohamady, S.; Desoky, A.; Taylor, S. D. Sulfonyl imidazolium salts as reagents for the rapid and efficient synthesis of nucleoside polyphosphates and their conjugates. *Org. Lett.* **2012**, *14*, 402–405.

[8] Sheldrick, G. M. SADABS. 1996.

[9] Sheldrick, G. M. Crystal structure refinement with SHELXL. *Acta Crystallogr. Sect. C Struct. Chem.* **2015**, *71*, 3–8.

[10] Sheldrick, G. M.; Schneider, T. R. *[16] SHELXL: High-resolution refinement*; 1997; pp 319–343.

[11] Spek, A. Single-crystal structure validation with the program PLATON. *J. Appl. Crystallogr.* **2003**, *36*, 7–13.